THE EFFECT OF EXCESS SURFACTANT REMOVAL ON THE THERMO-MECHANICAL BEHAVIOR OF EPOXY-CLAY NANOCOMPOSITES

By

CHAITANYA V. VISWANADHA

Bachelor of Technology in Mechanical Engineering
Jawaharlal Nehru Technological University
Hyderabad, Andhra Pradesh, India
2008

Submitted to the Faculty of the
Graduate College of
Oklahoma State University
in partial fulfillment of
the requirements for
the Degree of
MASTER OF SCIENCE
May, 2011

THE EFFECT OF EXCESS SURFACTANT REMOVAL ON THE THERMO-MECHANICAL BEHAVIOR OF EPOXY-CLAY NANOCOMPOSITES

Thesis Approved:

Dr. Raman P. Singh

Thesis Advisor

Dr. Kaan A. Kalkan

Dr. Sandip Harimkar

Dr. Mark E. Payton

Dean of the Graduate College

ACKNOWLEDGMENTS

Life will not be happy if one fails to achieve his goal. I take this a great chance to convey my gratitude to each and everyone who helped me in accomplishing my goal to pursue Master in Mechanical Engineering. I thank OSU for giving me the chance to study in one of the best educational institutions in the US. I thank my beloved advisor Dr. Raman Singh who has given me the opportunity to work with him starting as a teaching assistant and letting me to extend that further as research assistant. He is an amazing person who handles a bunch of people very enthusiastically with out any problems. I remember the days he inculcated the spirit in me when I was lagging concentration. I really thank him for comprehending the student and his personal situation, he made the phrase true i.e. "Singh is King."

I thank Dr.Kalkan and Dr.Harimkar who made their time flexible to the changing the defense dates and also for being my committee members. I thank Dr.Hanan and Masoud for being flexible with me in using the XRD machine.

My life as a research student will not be complete without thanking my peers Vasudevan (Yov Vasu) and Balaji (The Probably guy, The Lion). I was immensely influenced by their strategic approach towards problems and their solving techniques. Apart from being lovable room mates they were also very good lab mates. Leila–Masoud, were very helpful for all of us during our stay in Tulsa. Me with my roomies got the opportunity to taste a vast variety of Iranian dishes due to them. I thank Dr.Suraj Zunjarrao for sharing his ideas with me during my initial stage of research, his paper was a bible to me.

Seshumani, the most enthusiastic woman and the only person of my regional dialect has been very informative. She provided bundle of information when several questions

were introduced before her. I thank her for being helpful. Dhivakar, Chirag, and Arif (The three dudettes), my senior labmates and also very good friends have been very helpful and encouraging through the term of study. I cherish each and every moment I have spent with them. They are a medley of humor and knowledge. I thank you guys for your immense support. I thank Sadia (The Chatter box) and Sallah Uddin (The iPhone man) for being very co-operative in the lab and always welcomed me with a smile. Their are a sink for me when I was stressful. Thank you very much guys for your company for the years at OSU.

I thank my MAML friends Abhisek Jain (The stylish guy), Kunal Mishra (The POSS man, KYA BEY), Suman (The Genius), Philp Roger (Co-Clay guy), Austin, Dr. Nawani, Mohamad and Dr.Pandey for their support. I thank Dr. Ausman, Lawanya and Bastola for helping me on the TGA. I thank Bret for letting me use the machine shop during all the times. I thank my other roomates Krishna Chaitanya, Rengarajan for providing me stay in Tulsa and for helping me in the day-to-day life. I extend my wishes to Pradeep Gaddam (The Sleepy Boy, Vizag Boy)and Sai Kiran (The Photo Man, Mr. Makoman) for being very understandable and loving friends.

My thesis will not be complete without thanking the most important people of my life, they are Dad, Mom, and Sister who have been supporting me all through out the term of my study and understanding my situation and also I thank my fiancee Bhargavi for her presence and support over the phone for the past two years. I thank my brother Ranganath Panchangam and for his encouragement. I finally thank my cousin Viswakanth and all my best and beloved friends for their support and company.

TABLE OF CONTENTS

LIST OF TABLES

LIST OF FIGURES

CHAPTER 1

INTRODUCTION

1.1 Importance of Polymers Composites

Polymer composites have gained enormous importance in numerous applications like aircraft, automobile, sport, food, construction, fuel, and marine industries where strength and weight are major concerns. They are being used in wide range of applications due to their light weight, cost effectiveness, superior mechanical, barrier properties and resistance to chemicals when they are reinforced with materials called as fillers. It was found that when polymer composites were reinforced with fillers the strength of the composite improves from 20% to 200% depending on the kind of filler used [1].

These reinforcements can be either micro fillers or nano fillers. Some of the reinforcements are nylon 6 fibers [2–4], carbon fibers [5, 6], alumina particles [7–9], clay particles [10–15], Polyhedral Oligomeric Selsesquioxane (POSS) particles [16–18], core shell rubber particles [19], and carbon nanotubes [20–26].

Among all the above reinforcements, nanoclay is being widely used due to its sheet like structure (which helps in load transfer in resin), high stiffness, high aspect ratio, cost effectiveness, and provides superior mechanical, thermal, and barrier properties at low levels of loading when compared to neat resins. Due to less density and more number of the clay particles the polymer nanocomposites are light in weight compared to the traditional polymer composite materials that typically have a volume percentage of filler ranging from 30-60% [27]. In this work we try to study the mechanical and thermal properties of epoxy-clay nanocomposites when commercially available clays were subjected to excess surfactant removal.

1.1.1 Clay

Clay is a montmorillonite mineral belonging to the smectite family, obtained from the volcanic eruptions of bentonite. Clay structure has two tetrahedral rings sandwiching an octahedral ring which can also referred as 2:1. The octahedral ring is made up of aluminum oxide layer that has aluminum and magnesium ions inside the complex.

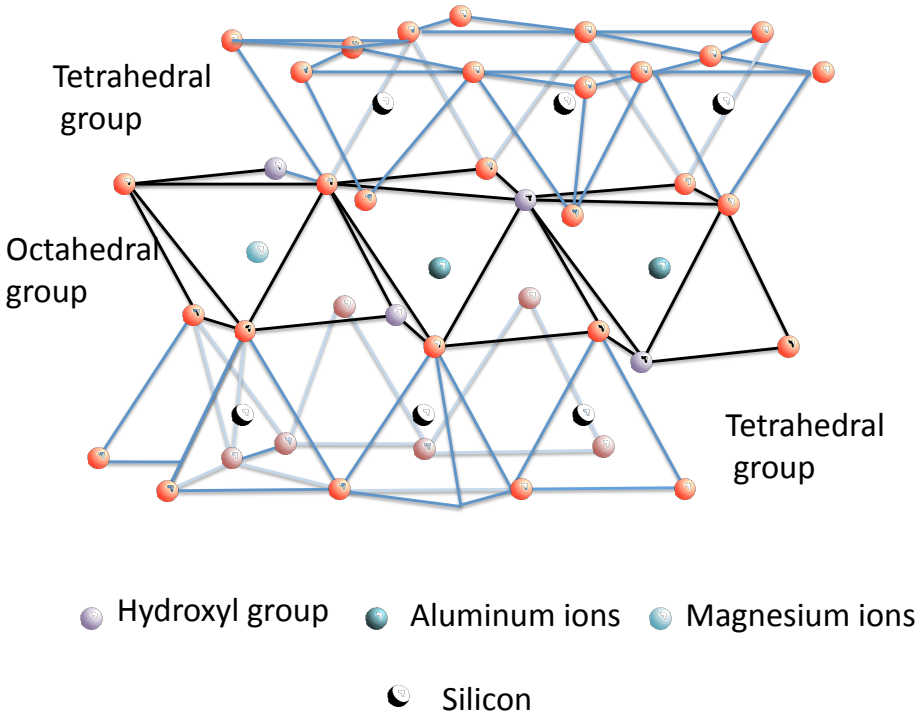

Figure 1.1: Structure of Montmorillonite

Due to the isomorphic substitutions between these aluminum and magnesium metal ions there is a negative valence created which is balanced by the sodium ion located on the clay surface. The clay platelets are stacked parallel (as observed in the figure 1.2) and separated by van der Waals forces and electrostatic forces. Fig. 1.2 clearly shows the clay platelets placed parallel to each other and separated by a certain distance. Clays deliver

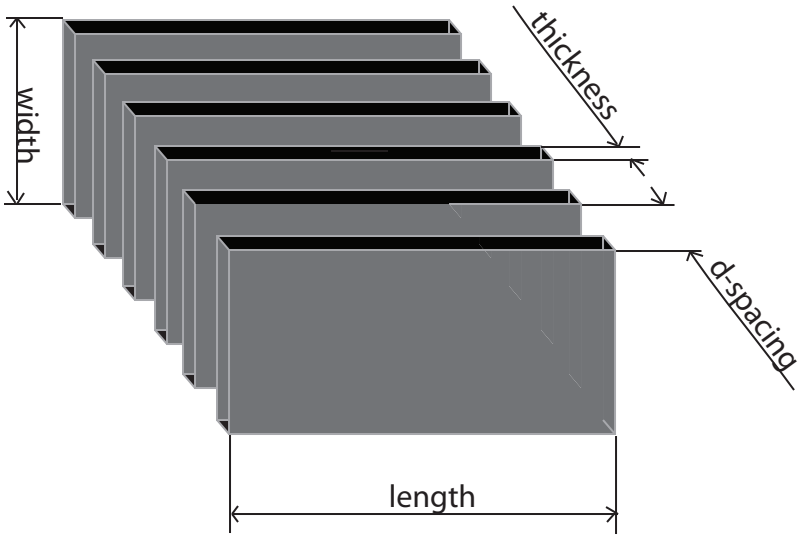

Figure 1.2: Clay platelet structure

high strength and stiffness due to their high aspect ratio which is the ratio of the square root of surface area of the platelet to the thickness (0.97nm). The d–spacing, thickness, length and width of the clay platelet are shown above. The d–spacing which is defined as basal spacing is the sum of the thickness of clay platelet and distance between two subsequent clay platelets [1].

1.1.2 Literature on polymer clay nanocomposites

It was discovered by Toyota that, incorporating low volume fractions of clay (such as 2%) with nylon fibers, improved the strength, modulus, and heat distortion temperature of the composite [28]. Leite $et.\ al.$ [29] worked with nylon fibers using clays which were treated with various ammonium salts. It was observed that the mechanical properties of the nylon-clay nanocomposite were improved compared to that of neat nylon polymer. Also it was noticed that the clay compatibility improved with polymer matrix providing an exfoliated structure that was shown as an improvement in the tensile modulus and yield strength with reduction in elongation. Weon and Sue [30], studied the effects of clay orientation and

aspect ratio, on mechanical properties of nylon 6 nanocomposites. It was noticed that with the reduction in the aspect ratio the modulus, strength, and heat distortion temperature were reduced but an improvement was found in the fracture toughness and ductility.

Han $et.\ al.$ [31], also worked on the treatment of organoclays with different ammonium acids and studied the effect of treatment on the mechanical properties of the nylon 6–clay nanocomposites. Lai and Kim [32] modified the surface of clay using epoxy and found an improvement in the d–spacing, thermal stability, mechanical properties, and gas-barrier characteristics of the poly ethylene terephthalate-co-ethylene napthalate (PETN) nanocomposites. Here the epoxy acted as a compatibilizer and chain extender in improving the interactions between the clay-resin and restricting the mobility of the molecular chain in the vicinity of the clay particles. This treatment showed a comparative improvement of strength and modulus of the composite. Shah and Paul [33], fabricated nylon 6-clay nanocomposites using melt mixing master-batch process technique to study the physical properties of low molecular weight nylon 6 nanocomposites in comparison to High Molecular Weight nylon 6 nanocomposites. It was observed that the clay introduction plays a key role in reducing the melt viscosity of the mixture and does not affect the performance of low molecular weight nylon 6 nanocomposites compared to the High Molecular Weight nanocomposites.

Clays are extensively used as a reinforcing agents in epoxies, elastomers, thermoplastic resins to improve mechanical properties like toughness, strength, and modulus [33-44]. Researchers reported that the addition of clay results in improved quasi-static fracture toughness [34], flexure modulus [35], elastic modulus [35], storage modulus [35], glass transition temperature [35,36], and reduced flexure strength as well as impact fracture toughness [34]. Zunjarrao $et.\ al.$ [37] reported an improvement in the fracture toughness and flexure modulus when clay volume was increased in nanocomposites. Composites were synthesized using high speed shear mixing and ultrasonic mixing and the maximum improvement was observed for composites made out of shear mixing. Abot $et.\ al.$ [38] observed that when clay was added to glass-epoxy composites, the elastic modulus of the system improved at

the expense of tensile strength and ductility along with reduction in glass transition temperature (T_g).

Researchers found a reduction in the moisture uptake of epoxy–clay nanocomposites [39]. Zainuddin $et.\ al.$ [40] worked on the water moisture uptake and variation in the mechanical properties with clay addition. It was noticed that the epoxy samples reinforced with clay displayed a great reduction in moisture intake. It is generally believed that the mechanical properties differ for a certain polymer nanocomposite due to the disparity in the surfactants or the curing agents that were used and the extent of curing of the composite. Sharma [41] reported 95% enhancement in the tensile strength, 152% increase in the tensile modulus, 87°C improvement in the thermal degradation temperature and 4°C improvement in the melting point with the surface modification of clay in polypropylene nanocomposites.

1.1.3 Dispersion of clay in polymer resins

The dispersion of clay in polymers (which are hydrophobic in nature) is a cumbersome process due to the hydrophilic nature of clay. The properties of a nanocomposite are governed by the extent of dispersion of the clay in the resin. Dispersion governs the properties of a composite material. Greater the dispersion, greater will be the contact area of the clay surface with the resin which enhances the load transferring capacity of composites there by increasing the mechanical, thermal and barrier properties. A lot of work was done by researchers in dispersing the clay in resin to achieve optimum properties. Zunjarao $et.\ al.$ [37] found that with change in the processing parameters and clay volume fraction the mechanical properties of composites varied. Ngo $et.\ al.$ [42] reported that the temperature, duration and speed of pre-mixing show an indirect effect on the formation of intercalated and exfoliated composites during the curing process. Generally dispersion is classified in to three terms: phase separation, intercalation, and exfoliation. Dispersion of clay in resin governs the properties of a composite. Phase separation or agglomeration is breaking of

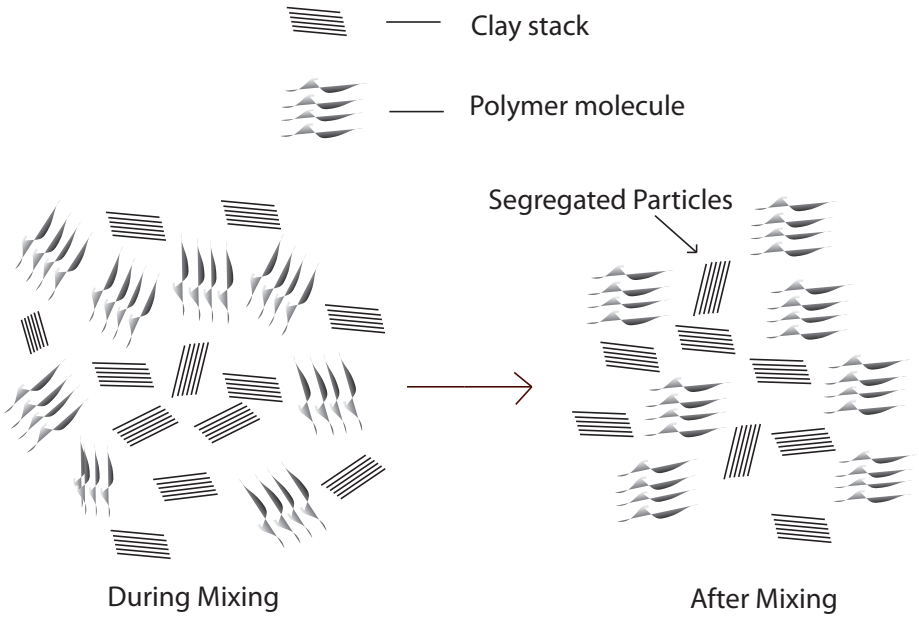

Figure 1.3: Agglomeration mechanism

clay tactoids or stacks in the resin with the tactoids having no monomer particle present in Fig. 1.3. Intercalation is breaking of clay stacks into groups of smaller stacks with galleries having monomer molecules shown in Fig 1.4. Exfoliation is the separation of the clay platelets into individual platelets in the polymer resin shown in fig 1.5 and it gives the best mechanical and barrier properties [1] .

Due to the hydrophillic nature of clay and hydrophobic nature of polymer its hard to develop an interaction between them. In order to achieve good dispersion the clay surface is modified with surfactants, which makes the clay galleries attractive for polymer molecules. The clay surface modification involves the substitution of the sodium ions on the clay walls with cations of surfactant which was clearly depicted in the fig. 1.6. The amount of cations exchanged with the sodium ions depends on the cation exchange capacity of the clay.

Modification of clay surface in the industries is done using salts of ammonium and phosphonium, as they were being widely used. The clays modified by ammonium salts are termed as ammonium modified clays or organoclays and those modified using phos-

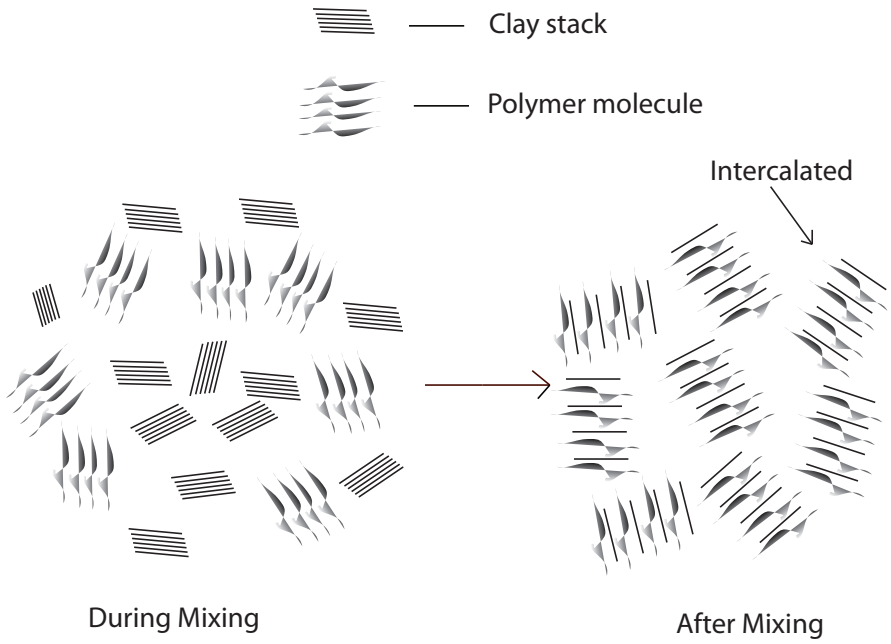

Figure 1.4: Intercalation mechanism

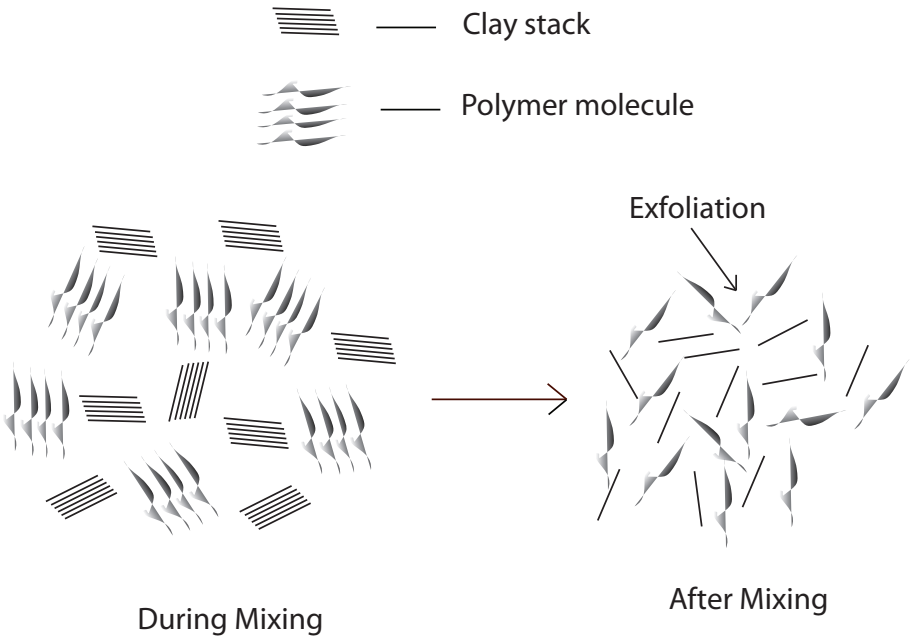

Figure 1.5: Exfoliation mechanism

phonium are called as phosphonium modified clays. Some of the organic surfactants are dimethyl dehydrogenated tallow quaternary ammonium salt and octadecyl trimethyl amine and few examples of phosphonium surfactants are ethyl triphenyl phosphonium salts, tributylphosphonium salts [43–46].

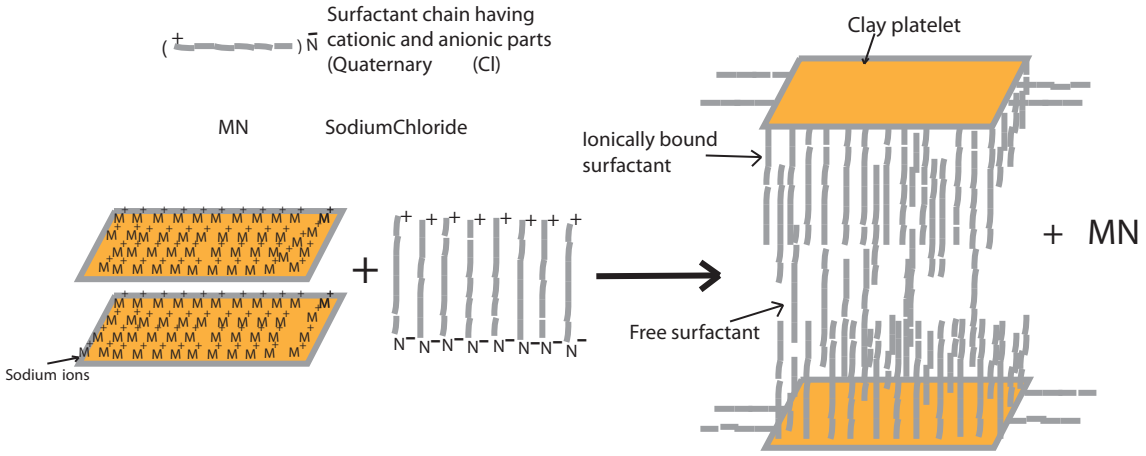

Figure 1.6: Clay modification using surfactant

1.1.4 Literature on excess surfactant

The clay galleries are over-saturated with excessive surfactant in order to modify the surface, during this process some amount of surfactant will be loosely bound or chemically gets adsorbed to the walls of the clay platelets in fig 1.7. This kind of surfactant is less stable in nature and decomposes at lower temperatures compared to the ionically bound surfactant [45]. The degradation of specific clay depends on the corresponding surfactant present in the clay galleries. Ammonium surfactants have very low thermal degradation temperature of 160–220°C whereas phosphonium surfactants have a thermal degradation temperature around 280–350°C [46]. Li $et.\ al.$ [47] stated that the surfactant will be freely grafted, adsorbed on the surface of the clay platelet. The thermal degradation temperature of the as-received or free surfactant was less than that of ionically bound clay. Earlier, re-

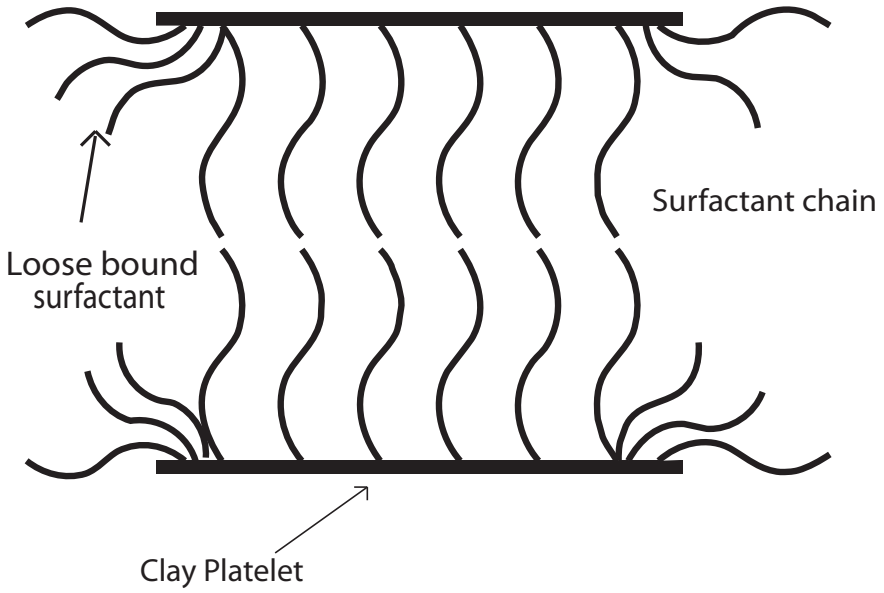

Figure 1.7: Clay with strong and dangling surfactant chain

searchers worked on the removal of excess surfactants from the clay galleries and studied the resultant mechanical properties of their nanocomposites.

Cui $et.\ al.$ [45] worked on the excessive surfactant removal at isothermal conditions using TGA and found that the thermal degradation temperature of the clay improved with the removal of the excess surfactant. This improved clay was incorporated in polypropylene composites for studying the change in the mechanical properties and it was found that washing did not affect the mechanical properties [48]. Morgan and Harris [49] studied the effect of removal of excess surfactant on the organoclay using soxhlet extraction process. It was found that the flexural modulus and dispersion were improved with lowering of heat release rate and delayed time to ignition of polypropylene nanocomposites. Nawani $et.\ al.$ [50] reported a remarkable improvement in the thermal degradation temperature of clay by removing the dangling surfactant and modifying the clay surface using transition metal ions.

Park and Jana [51] reported that the excessive surfactant affected the curing kinetics of the epoxy-clay composite. It was mentioned that the excessive diamine of the curing agent caused plasticization in the epoxy networks and lowered the values of inter-gallery modulus. Carrasco and Pages [52] using TGA and FTIR studies found that, addition of nanoclay accelerates the curing rate of the composite. The collisions of the resin molecules within the galleries were less as they there were protected by the galleries against thermal degradation compared to those outside the galleries. While, researchers have investigated the effect of washing on the impact and tensile properties, there is no information available regarding the effect of washing on the quasi-static fracture toughness of polymer-clay composites which is the primary focus of this study.

CHAPTER 2

MATERIALS

2.1 Materials & Methods

We are interested in comprehending the behavior of a resin (matrix) system, when reinforced with washed (thermally improved clay) clay. The resin chosen for this work is Epon 862 (Hexion speciality chemical, Columbus, OH, USA). The reason for choosing this particular epoxy resin is because, it is a well-understood resin in DGEB-F system and provides superior mechanical properties at lower viscosities. A low viscosity aliphatic amine Epikure 3274 (Hexion speciality chemical, Columbus, OH, USA) wa used as a curing agent.

Commercially available clays such as, Cloisite 20A (Southern Clay Products, Gonzales TX, USA) having average particle of 2-13 μm and Nanomer I.28E (having an aspect ratio of 75-120) which are montmorillonites having an average particle size of 8-10 μm modified with dimethyl dehydrogenated ditallow quaternary ammonium salts and quaternary trimethylstearyl ammonium salts respectively were used. The above clays were chosen due to their resistance to high temperature and compatibility with the resin. Researchers [53] stated that the cation exchange sites for the Cloisite Na^+ MMT were less when compared to the Na^+ PGW of Nanocor. However, the ion exchange of the Cloisite clays were of the order 110-150% whereas of the Nanocor clays was 93%. They reported that by studying the weight % of organic part in the clay i.e., Cloisite clays was greater than Nanocor clay which means that the Cation Exchange Capacity of Cloisite clays (110–115% ion exchange which indicates the overloading of surfactant) was higher compared to Nanocor clays (93-95% degree of ion-exchange). However when taken to the cation exchange capacity of

their respective clay, both of the clays are having same amount of surfactant.

Methanol (VWR International, West Chester, Pennsylvania, USA) was used as a solvent for washing clay and silver nitrate (VWR International, West Chester, Pennsylvania, USA) was used for detection of surfactant in the filtrate. Magnetic stirrer (VWR International, Ceramic top, Volts 120VAC, Watts 900, Frequency 50/60 Hz, Heat 0–500°C, and @ 01600 rpm, USA) was used for mixing the clay in epoxy. A high speed shear disperser (T-25 ULTRA TURRAX with SV 25 KV25 F dispersing element, IKA Works Inc., Wilmington, North Carolina, USA) was used for post mixing the epoxy with clay. Filter paper (VWR International, West Chester, Pennsylvania, USA) having a refining size up to 5μm was used for filtering the clay from methanol.

Details	**Resin**	**Curing Agent**
Name	Epon 862	Epikure 2374
Chemical nature	Di–glycidyl ether of bisphenol–F (DGEB–F)	Low viscosity Aliphatic amine
Curing cycle	Pre-curing: 24 hrs at room temperature	Post-curing: 6 hrs at 121°C
Stress Intensity	1.1 MPam$^{1/2}$	–
Density	1.17 gm/cc	–

Table 2.1: Table showing properties of resin and curing agent

2.1.1 Washing of clay

Lagaly and Malberg [54] reported that disarticulation of pure clay is very easier in water due to the hydrophobicization of the clay surface. They added that organoclay disaggregation increases in the order of cyclohexanes (having no disarticulation), alcohols, cyclohexanones (ketones), formamides and reaches the highest degree with nitrobenzene. Tran $et.\ al.$ [55], from a detailed study noticed that the dispersion of organoclays is more in the R$_n$OH alcohols with n more than 4. This explained that alcohols technically with lower

Details	Cloisite 20A	Nanomer I.28E
Manufacturer	Southern Clay Products	Nanocor Industries
Surfactant	2DM 2HT	Trimethyl stearyl
Avg particle size	2-13μm	8-10μm
Color	Slight yellow	White
Base clay	Na^+	Na PWG

Table 2.2: Table showing details of both the clays used in the work

2DM2HT – Dimethyl dihydrogenated tallow quaternary ammonium salt

chain (e.g. methanol, ethanol, propanol, butanol) cannot disperse the clay particles due to more polarity and hydrogen bonding which reduces subsequently with the increase in the chain size.

Earlier, it was reported [45] that washing of clay using methanol was an effective technique to remove the loosely bound surfactant. The previous studies led us to choose methanol as a solvent for this study. Three grams of clay was added to 50 grams of methanol and stirred at 700 rpm for 1 hour on a magnetic stirrer and the solution was allowed to settle down for 10–15 minutes as shown in Fig. 2.1 a., b. The top clear solution of the methanol was filtered using a vacuum filtering setup (fig. 2) and fresh methanol was added to the mixture and this process was repeated three times [45].

2.1.2 Sample fabrication of as-received and washed clay with epoxy resin

A required amount of epoxy resin was pre-heated to 65°C in order to make it less viscous and desired weight fraction of clay was added to the epoxy and stirred for 12 hours at 65°C using magnetic stirrer followed by shear mixing adopting the same working parameters as reported by researchers [37]. It was found that shear mixing technique resulted in exfoliation and higher mechanical properties when compared to the ultrasonic mixing

using the same resin. The disparity between the two studies was due to the different surfactant in the clay. This mixing will induce huge amount of air bubbles in the resin which were removed through continuous degassing overnight. Curing agent was added to the resin in a proportion of 100:40 and hand mixed for 10 minutes followed by degassing to remove any entrapped air bubbles during mixing process. The epoxy-clay, curing agent mixture was casted into a 6 x 6 inch aluminum mold with PTFE sheet (Teflon) on its face and polyurethane strips at the edges. The sample fabrication procedure was same for the washed clay epoxy composites. The samples for testing were machined using high speed table saw cutter, for fracture sample the notch was made with the diamond saw cutter having a diamond blade.

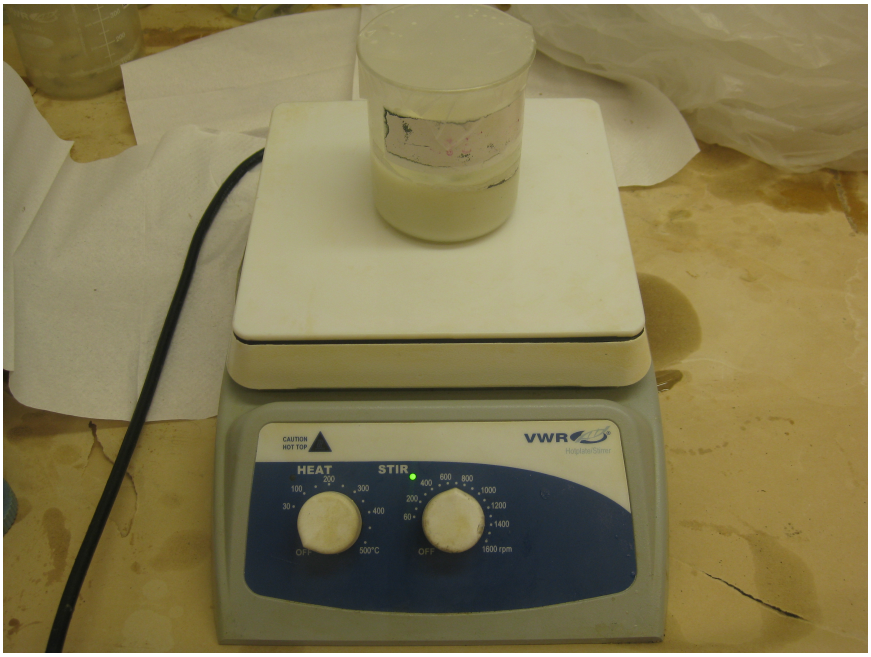

(a) Clay washed in methanol using magnetic stirrer

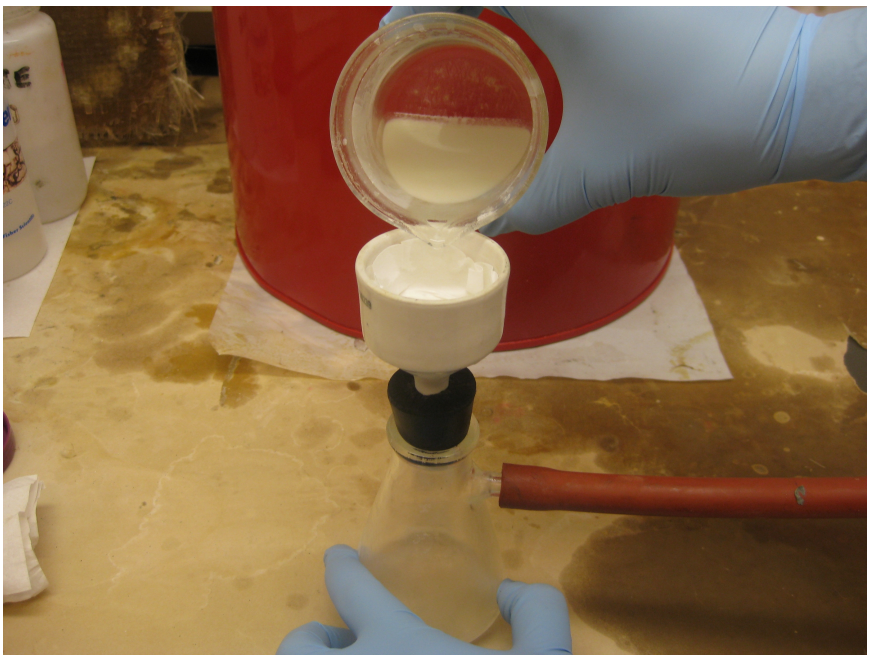

(b) Clay with methanol being filtered using vacuum filtering

Figure 2.1: Washing Process

CHAPTER 3

EXPERIMENTAL

3.1 Silver Nitrate Test

Silver nitrate was used to detect the presence of the surfactant. The methanol was filtered from the clay-methanol mixture in three stages and further added to silver nitrate. This addition of silver nitrate yields a precipitate from the methanol mixture.

3.2 Thermal Characterization

Thermo-Gravimetric Analysis was carried out to study the degradation pattern of both as-received and washed clays along with those of reinforced into resin. The temperature protocol was from 40-700°C with a ramp rate of 10°C/min. The thermal degradation graphs of the clays and their corresponding resins were studied using Mettler-Toledo instruments.

3.3 X-Ray Diffractometry

X-Ray Diffraction was carried out to measure the dispersion of clay in the polymers as shown in Fig. 3.1. Diffraction was performed in reflection using 0.3 mm collimator and Hi-Star 2D area detector on a Bruker D8 Discover diffractometer under Cu-Kα, 40 kV/40mA with a fixed incident angle of 5. Exposures were 60 s/frame under XY stage oscillation with 0.5 mm amplitude. The X-Ray diffractometer used for this work was a Wide angle X-ray machine (WAXD) with copper light source having a wavelength of λ=0.154 nm, operated at a voltage of 40KV and 40mA.

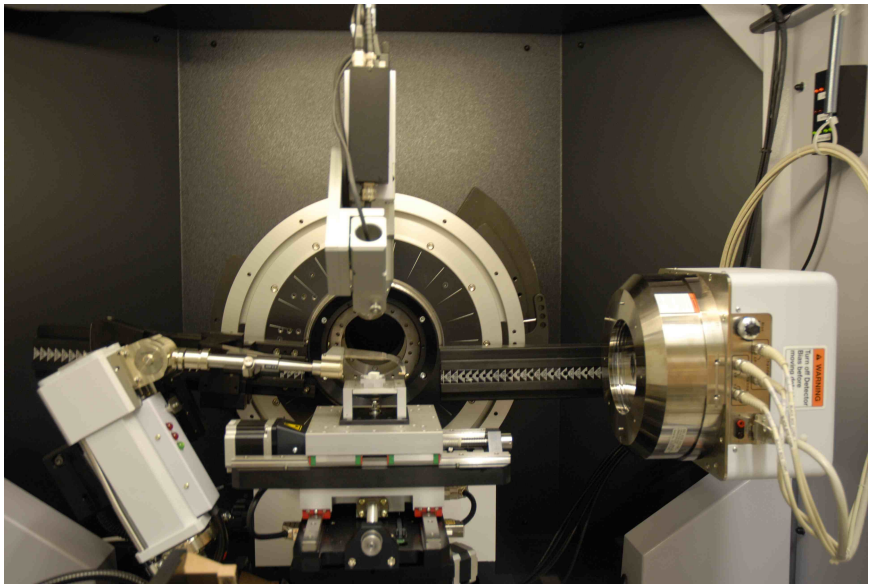

Figure 3.1: XRD carried out on a sample

3.4 Mechanical Property Characterization

3.4.1 Fracture toughness

Fracture toughness testing was carried out as per the ASTM 5045, also called as Single Edge Notch Bend test [56]. The samples were quasi-statically loaded by a universal testing machine at a loading rate of 0.5 mm/min with a span length of 2.0 inches. An overhanging length of 2.54 mm was retained on both the sides, as shown in Fig. 3.2. The dimensions of the samples were 54.00mm x 12.70mm x 6.35mm. A notch was cut using a high speed diamond saw cutter (MK-370, MK Diamond Products Inc., Torrance, California, USA) and the starter crack was introduced using a sharp razor blade. The length of the crack was measured with the use of an optical microscope, which has a traveling plate with graduations. The fracture toughness was calculated using the formula as shown in the below equation :

$$f(\frac{a}{W}) = \frac{3\frac{S}{W}\sqrt{\frac{a}{W}}}{2(1+2\frac{a}{W})(1-\frac{a}{W})^{\frac{3}{2}}} \times [1.99-(\frac{a}{W})(1-\frac{a}{W})(2.15-3.93\frac{a}{W}+2.7(\frac{a}{W})^2)] \quad (3.1)$$

Where, a = crack length, (in), K_{Ic} = stress intensity factor, (MPa $\sqrt{m}$), P_{max} = maximum

Figure 3.2: Fracture test carried on a specimen

load taken by the composite, (N), B = thickness of the specimen, (in), W = width of the specimen, (in) and $f(\frac{a}{W})$ = geometric stress intensity factor.

3.4.2 Flexure test

Three-point bend test as per ASTM D 790–07 was conducted to determine flexural properties of structural laminates such as maximum flexural strength and flexural modulus. Samples with dimensions, support span-to-depth ratio 16:1 were cut using table saw cutter and polished further considering the overhang length of 10 percentage of the support span. But in any case a minimum of one-fourth inch of overhang distance should be maintained as shown in fig. 3.3. The dimensions of the sample were 53.3mm x 12.7mm x 3.175mm, tested at a loading rate of 0.2 mm/min [57].

The finished samples are then placed in the 3 point bend test setup and the upper nose is set to touch exactly at the top of the specimen surface. Finally the load was applied with a particular rate of cross head motion which was obtained from the following formula:

$$R = \frac{ZL^2}{6d} \tag{3.2}$$

where R = rate of crosshead motion, mm (in.)/min, L = support span, mm (in.), d

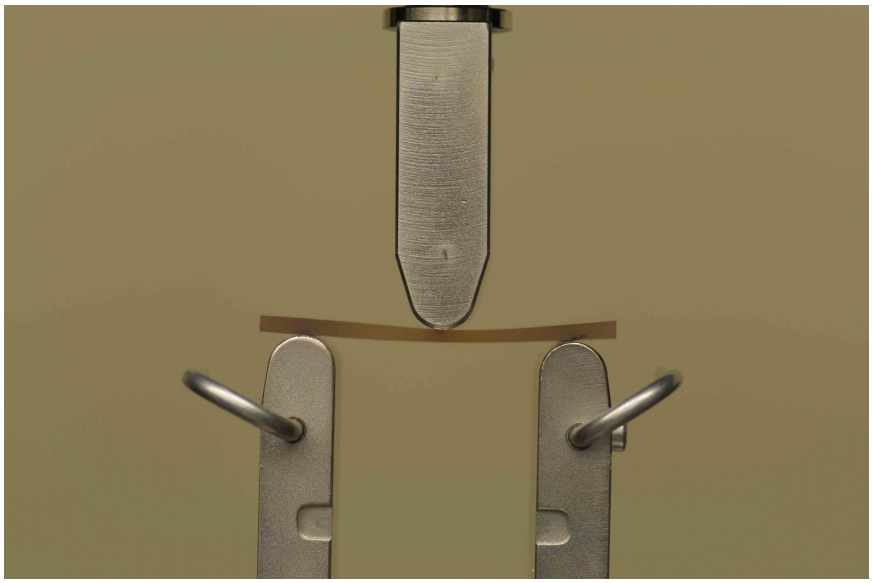

Figure 3.3: Flexure test carried on universal testing machine

= depth of beam, mm (in.), and Z = rate of straining of the outer fiber, mm/mm/min (in./in./min). $Z \simeq 0.01$

The load versus displacement was measured and a graph was drawn using the points obtained throughout the specimen testing. For determining maximum flexural strength, the maximum load obtained in the graph was considered. The following formula gives the maximum flexural strength of a specimen when subjected to a three point bending moment.

$$\sigma_{f\text{max}} = \frac{3P_{\text{max}}L}{2bd^2} \tag{3.3}$$

where, σ = stress in the outer fibers at midpoint, MPa (psi), P_{max} = maximum load obtained in the load-deflection curve, N (lbf), L = support span, mm (in.), b = width of beam tested, mm (in.) and d = depth of beam tested, mm (in.)

The flexural modulus of the specimen is the ratio of flexural stress to corresponding flexural strain when considered within the elastic limit. It was calculated using the following general formula, where the slope m, was found by considering the steepest initial line on the load deflection curve.

$$E_B = \frac{L^3 m}{4bd^3} \tag{3.4}$$

where, E_B = modulus of elasticity in bending, MPa (psi), L = support span, mm (in.), b = width of beam tested, mm (in.), d = depth of beam tested, mm (in.), and m = slope of the tangent to the initial straight-line.

3.5 Scanning Electron Microscope imaging

The morphology of the fractured samples were analyzed using the Scanning electron microscope (SEM) of (Hitachi S-4800 FESEM, Dallas, TX). The samples since being non conductive were sputtered using the gold-palladium alloy metal before any imaging was done. The sputtered samples were used for further imaging.

CHAPTER 4

RESULTS AND DISCUSSION

4.1 Silver Nitrate Test

The removal of surfactant was confirmed by performing silver nitrate test. When $AgNO_3$ was added to the filtrate containing trapped chloride ions of the surfactant a white precipitate results due to the reaction between Ag^+ and Cl^- ions. When the filtrate obtained after the washes was treated with $AgNO_3$, a white precipitate appears confirming the removal of surfactant from the clay.

C 20A: When pure methanol was added to 5 grams of silver nitrate solution no precipitate was observed as expected, however a white precipitate was observed when it was added to the filtrate obtained on washing with methanol for three times. This white precipitate confirms the loss of free surfactant, this was further confirmed from the TGA curves discussed later in this work.

I.28E: After the first wash of the clay, the color of the solution changed to slight white, forming a precipitate. With the subsequent washing of the clay, the precipitate formation was reduced. There was no appreciable change in the solution after the third wash. This shows that most of the excess surfactant has been removed during the first three washes.

4.2 Thermal Characterization of Clay and Their Epoxy Nanocomposites

Thermo-gravimetric analysis was carried out to study the degradation pattern of the organoclay and corresponding as-received and washed nanocomposites.

4.2.1 Thermo-gravimetric analysis of Cloisite 20A and their epoxy composites

Clay when subjected to thermo-gravimetric analysis, showed an improvement in the decomposition temperature and reduction in the heat release rate with washing. Figure 4.1 shows the degradation pattern of as-received and washed clay. The degradation initiated at 50°C and ended at 700°C. There was a clear shift in the graphs with variation in the weight% of clay. The end of the curve (around 700°C) indicated loss of material, which was attributed to the loosely bound surfactant. The reduction in the weight loss for the as-received clay was more compared to the washed clay. Washing improved the degradation temperature by 10–12°C . From the plots it was clear that the thermal stability of the clay was improved.

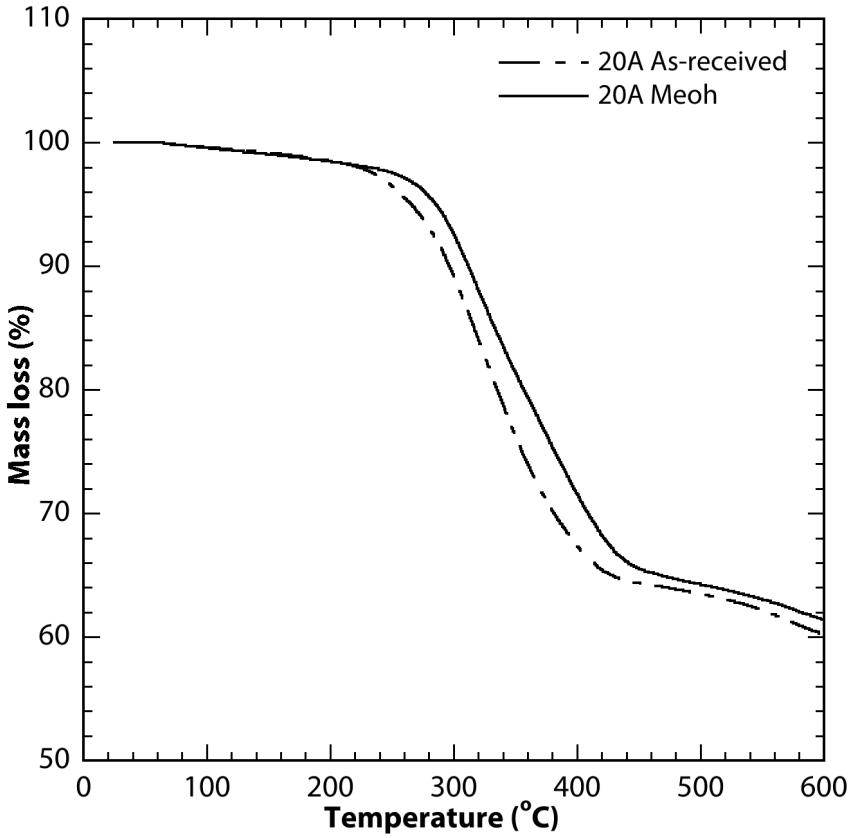

Figure 4.1: TGA of as-received and washed clay

Figure 4.2 shows the DTG curves where we can notice the loose bound surfactant being

removed during the washing process. A bump was clearly noticed around 230–280°C for as-received clay which was due to the presence of loose bound surfactant and not observed in the washed clay curves. This informs that most of the excess surfactant was driven out from the clay galleries after the third wash. The initiation of the grafted surfactant degradation was shown around 300°C and lasted till 410°C. This conveys that the excess surfactant removal causes slight improvement in stability of the clay.

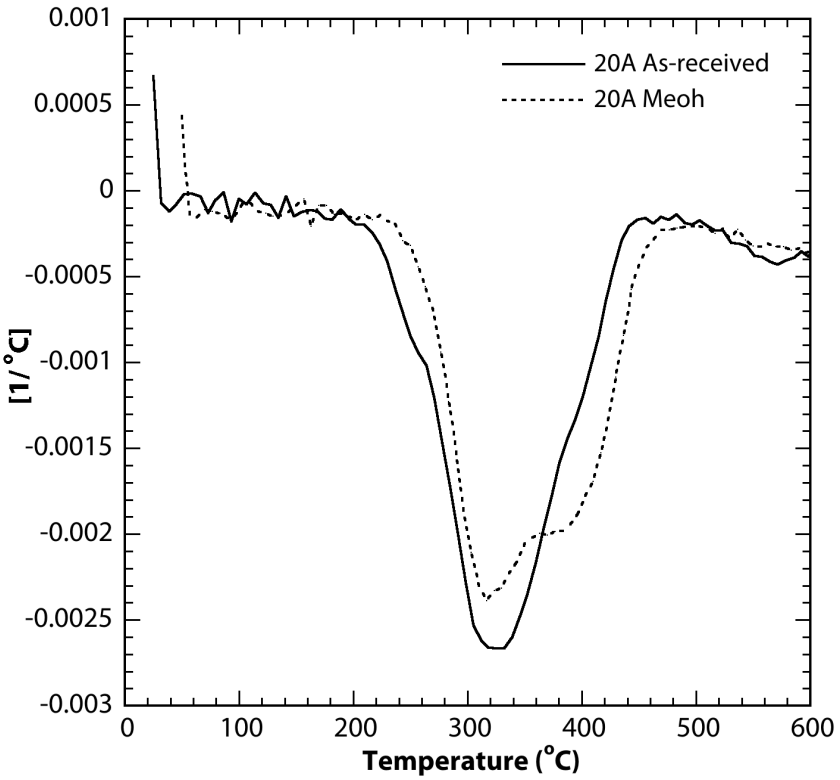

Figure 4.2: First derivative curves of as-received and washed clay

Figure 4.3 shows the mass–loss curves of as-received clay and the washed clay reinforced in epoxy resin. There was a slight improvement in the degradation of the washed epoxy-clay composite. During the initial stages in the case of the methanol washed epoxy-clay nanocomposites there was relatively more mass-loss compared to the as-received epoxy-clay nanocomposites. This might be the residual solvent trapping in the clay galleries during washing process. When this residual solvent was degraded it was observed that the degradation profile improved slightly. However the observed variation in the im-

provement was very less.

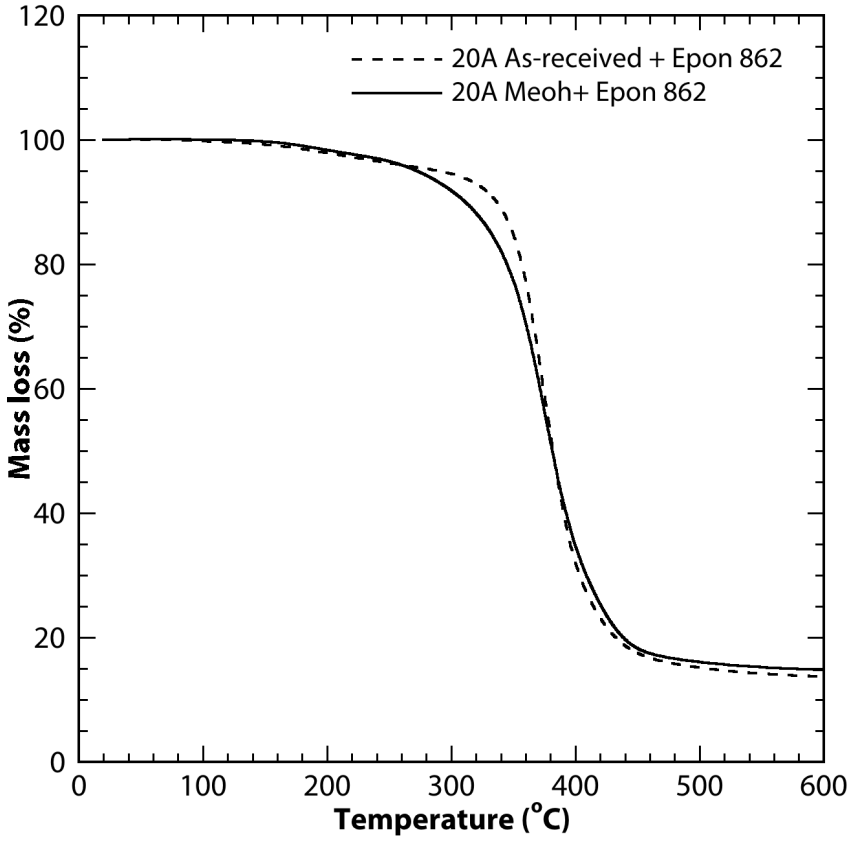

Figure 4.3: TGA curves of as-received and washed clay in resin

4.2.2 Thermo-gravimetric analysis of Nanomer I.28E clay and their epoxy composites

Figure 4.4 shows the TGA graph of the as-received clay and clay washed with methanol. When taken a look at the degradation pathway it can be noticed that there was a shift in the degradation lines to higher temperatures indicating that for a given temperature the mass loss was reduced. This implies that the amount of material decomposing at a given temperature was relatively less. The on-set of decomposition temperature was also improved which can be observed from the nose which falls at a range of 180–240°C for as-received clay and 220–280°C for washed clay. The shift in both the curves at the end-set of decomposition explained the loss of material which was removed in the form of loose surfactant.

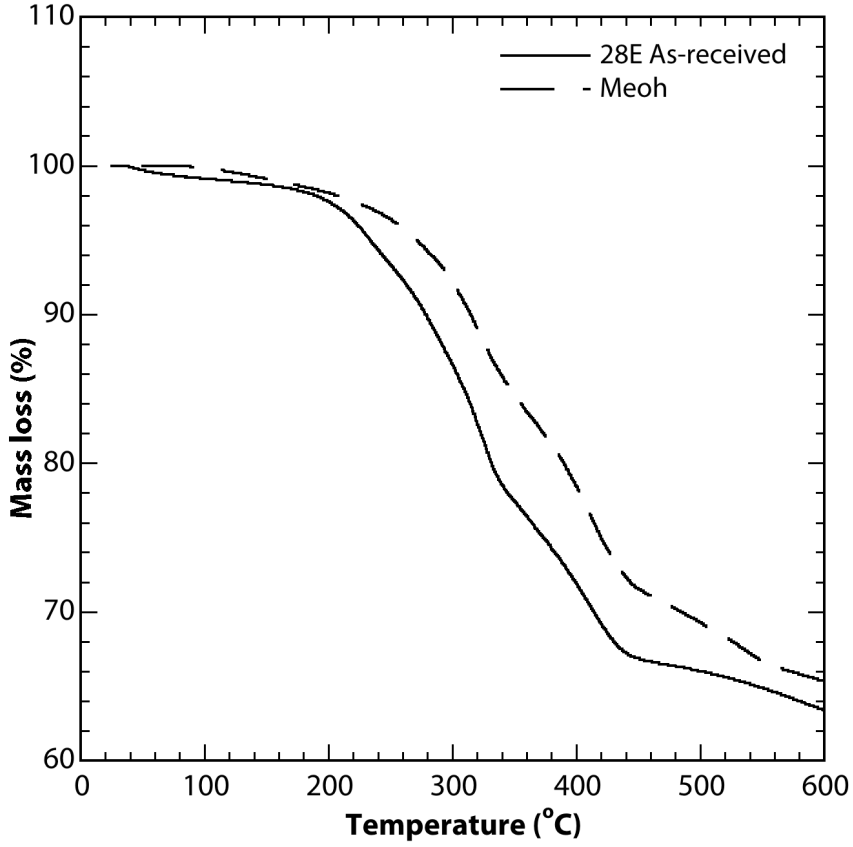

Figure 4.4: TGA of as-received and washed clay

The first derivative graphs (DTG) in fig. 4.5 shows the degradation pathway. Similar to the mass loss curves, the washed clay derivative curve displayed a shift from the as-received clay derivative plot. When carefully observed, there was a small protrusion in the as-received clay graph (around 180–280°C), which could not be observed in the methanol washed clay derivative graph. This was the free surfactant that degrades at a temperature range of 180–280°C. There was no significant variation in the maximum degradation temperature. The graphs displayed a complex two-stage degradation pattern which might be the degradation of the ionically bound surfactant at 320°C and the end of the total surfactant degradation at 420°C.

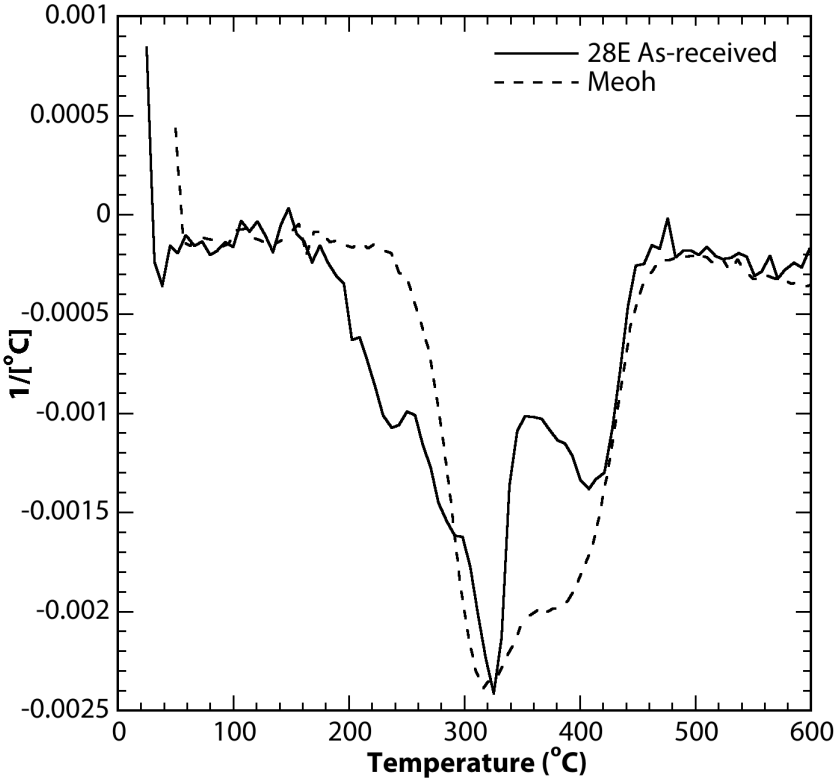

Figure 4.5: First derivative curves of as-received and washed clay

Figure 4.6 shows the graph for degradation of clay reinforced in epoxy. The nanocomposites with as-received clay displayed onset of degradation pattern approximately starting at 260°C and the decomposition reached the maximum around 600°C where the hydroxyl part will be lost making the structure imbalanced. The degradation curve of the nanocom-

posite with methanol washed clay was also plotted to study the difference in the degradation pattern.

During the initial stage of degradation, it was observed that the mass loss in the washed nanocomposite was more than the as-received nanocomposite from the fig. 4.6. This might be due to the residual solvent methanol trapped inside the galleries of the clay during the washing process which degrades during the initial stages which was similarly observed in the case of 20A epoxy-clay nanocomposites. When this residual solvent was decomposed a slight improvement in the stability of the graph was observed.

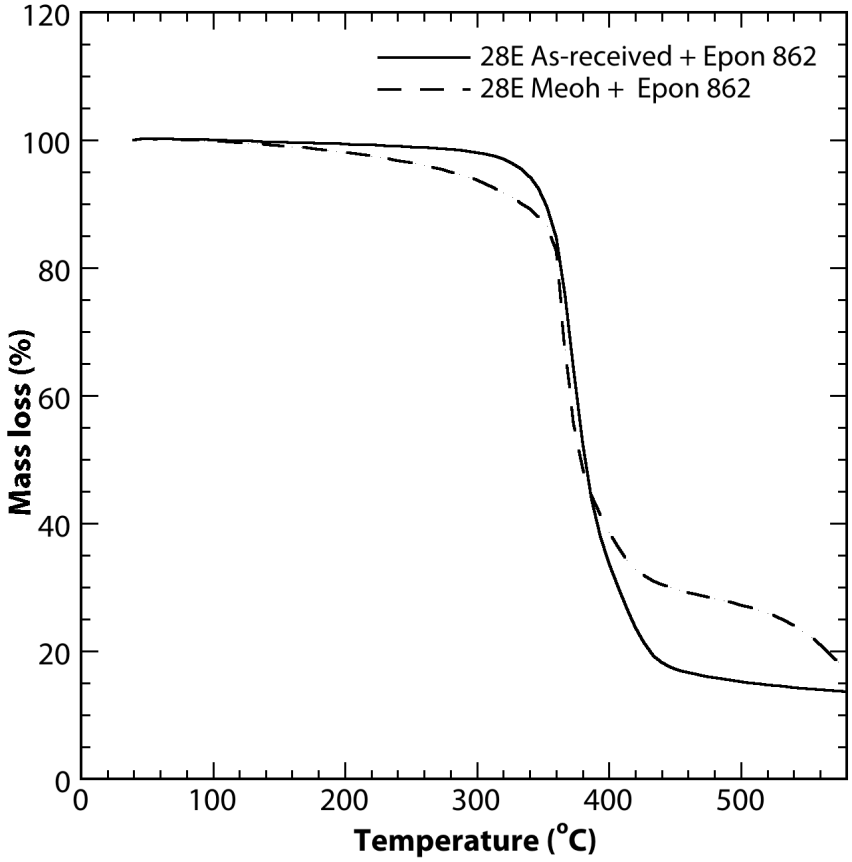

Figure 4.6: TGA curves of as-received and washed clay in resin

4.3 X-Ray Diffraction Analysis

4.3.1 X-ray analysis of Cloisite 20A clay and their epoxy nanocomposites

Figure 4.7 shows the diffractograms of different clay weight fractions of the nanocomposites. The highest peak in the plot was the characteristic of the as-received clay. There were prominent peaks observed for 0.25 wt%, 0.5 wt%, 1.0 wt% and 2.0 wt% of epoxy-clay nanocomposites. These peaks correspond to the partial intercalation of clay in the epoxy-clay nanocomposites. The d-spacing of the characteristic clay peak was noticed at 2.45nm. When the clay was reinforced in the resin the d-spacing was improved from 2.45 nm to 3.39 nm (for 2.0 wt%) and 3.52 nm (for 0.25 wt%, 0.5 wt%, 1.0 wt%). Table 4.1 shows the XRD data for the as-received clay and nanocomposites.

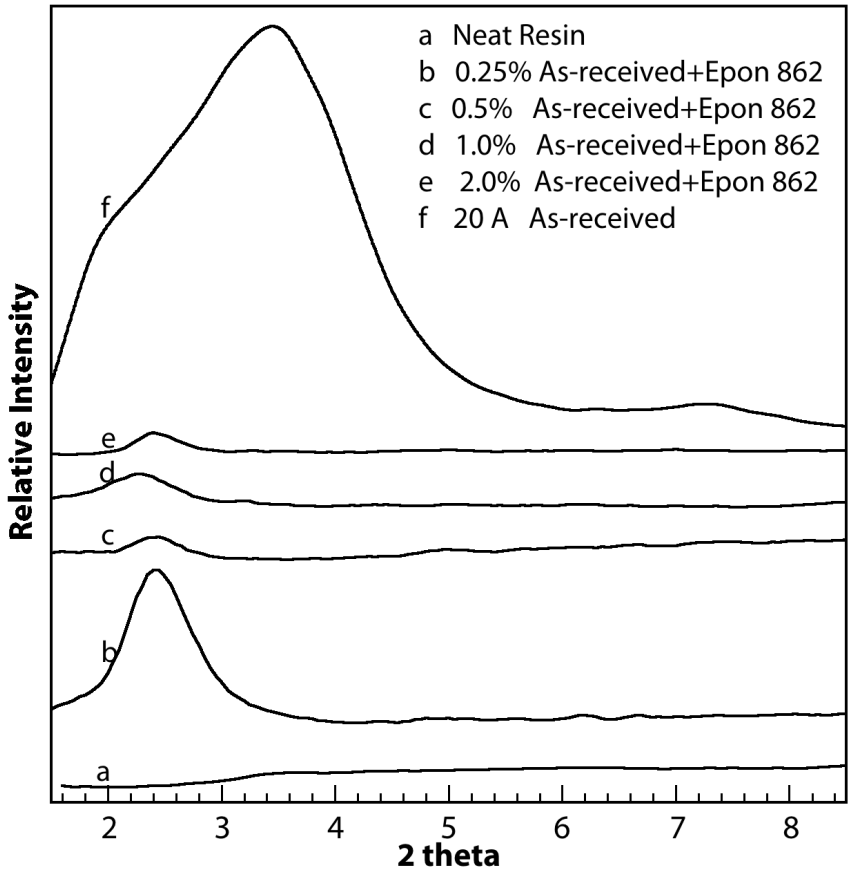

Figure 4.7: XRD curves of as-received clay and their respective nanocomposites

Weight % of clay	**(2θ) (001)**	**(2θ) (002)**	**d(nm) (001)**	**d(nm) (002)**
As-received clay	3.6	7.2	2.65	1.22
0.25	2.5	–	3.52	–
0.5	2.5	–	3.52	–
1.0	2.5	–	3.52	–
2.0	2.6	–	3.39	–

Table 4.1: XRD data for the as-received clay nanocomposites

The diffractograms for the washed 20A clay were shown in the fig. 4.8. There was a reduction in the d-spacing of the washed clay as expected due to the removal of lose bound surfactant from the galleries. The peak was observed around 4.1^o which has a d-spacing of 2.2 nm. The clay loaded nanocomposites displayed an improvement in the d-spacing of 3.39 nm (for 2.0 wt%) and 3.52 nm (0.25wt% and 1.0 wt%). The 0.5 wt% clay loaded nanocomposite did not show any presence of peaks indicating a disordering of the clay stacks in the resin. Table. 4.2 shows the XRD data for the methanol washed clay and their corresponding epoxy nanocomposites.

Weight % of clay	**(2θ) (001)**	**(2θ) (002)**	**d(nm) (001)**	**d(nm) (002)**
Methanol washed clay	4.1	7.6	2.2	1.16
0.25	2.5	–	3.52	–
0.5	Nill	–	–	–
1.0	2.5	–	3.52	–
2.0	2.6	–	3.39	–

Table 4.2: XRD data for the methanol washed clay nanocomposites

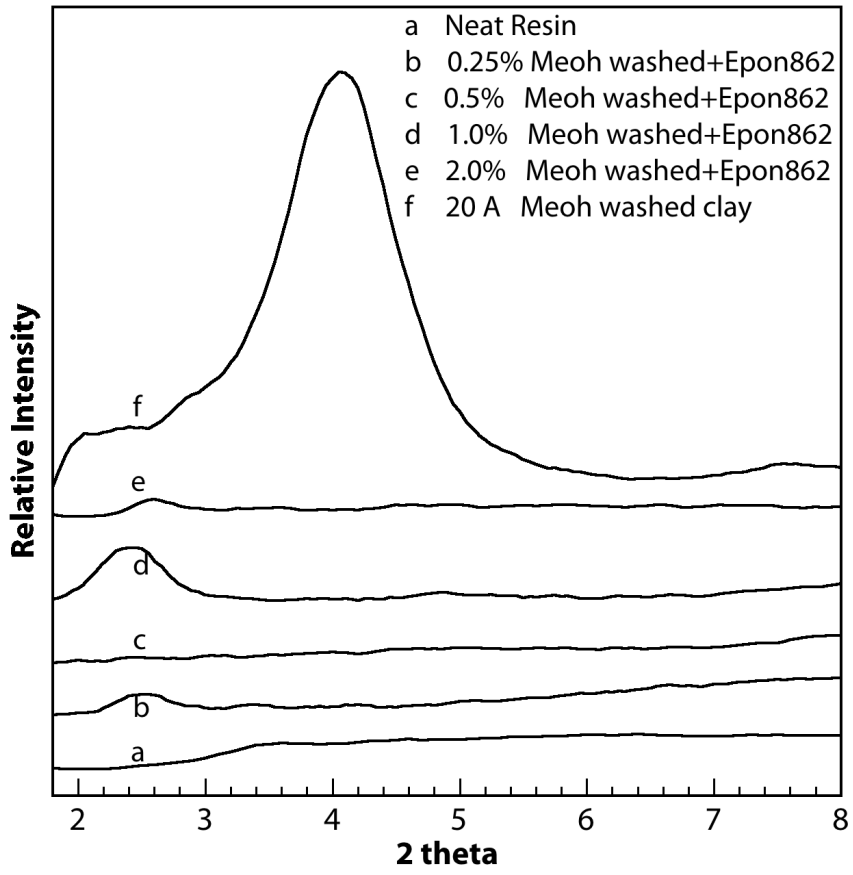

Figure 4.8: XRD curves of washed clay and their respective nanocomposites

4.3.2 X-ray analysis of Nanomer I.28E and their epoxy nanocomposites

The XRD plots 4.9 and 4.10 of the as-received and washed clay were informative in regards to the ordered clay peaks which were formed as a result of the shear mixing process. The neat resin did not exhibit any peaks. The as-received clay displayed peak at 3.8° which corresponds to a d-spacing of 2.32 nm. The peak related to 0.5 wt% clay composite indicated a reduction in the d-spacing. The resin loaded with 1.0 wt% clay exhibited a peak at 2.5° corresponding to the basal plane (001) with a d-spacing of 3.52 nm and also a peak at 4.8° for (002) basal plane having a d-spacing of 1.84 nm indicating agglomeration. The 2.0wt% clay nanocomposite did not display the primary peak but exhibited a peak at 4.8° which was caused due to the agglomeration of the clay. Table 4.3 shows the XRD data for the as-received epoxy-clay nanocomposites.

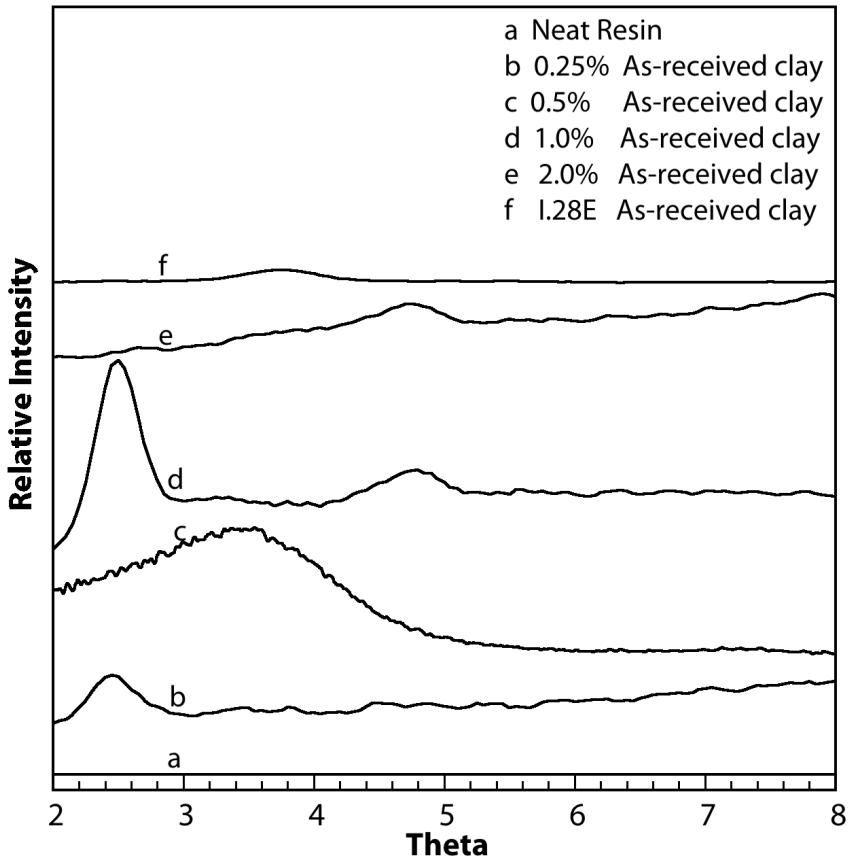

Figure 4.9: XRD curves of as-received clay and their respective nanocomposites

Weight % of clay	**(2θ) (001)**	**(2θ) (002)**	**d(nm) (001)**	**d(nm) (002)**
As-received clay	3.6		2.45	–
0.25	2.5	–	3.52	–
0.5	3.4	–	2.59	–
1.0	2.5	4.8	3.52	1.84
2.0	–	4.8	–	1.84

Table 4.3: XRD data for the as-received clay nanocomposites

XRD of the washed clays was plotted in the Fig. 4.10. The characteristic peak of 28E clay shifts to higher angles indicating a reduction in the gallery spacing. This was evident from the fact that removal of free (unexchanged) surfactant reduced the d-spacing pushing the galleries closer. Nanocomposites fabricated out of 0.25 wt% and 0.5 wt% clay were observed to have the peak at 2.4° which corresponds to a d-spacing of 3.59 nm. Unlikely, the peak of 1.0 wt% clay nanocomposite was shifted right indicating an increment in the angle 2.6° (d-spacing of 3.39 nm) and reduction in the d-spacing. The 2.0 wt% clay nanocomposites showed a peak at 2.5° with a d-spacing of 3.52 nm. Nanocomposites fabricated out of 1.0 wt% and 2.0 wt% clay displayed secondary peaks which were due to the result of agglomeration. This might be due to the very less or no free surfactant, which drives the monomer molecules into the clay galleries. Table 4.4 shows the XRD data for the methanol washed clay and nanocomposites.

Xidas and Triantafyllidis [53] studied the effect of surfactant type and clay structure on the thermal and mechanical properties of glassy, rubbery-epoxy nanocomposites. It was realized that the interactions between the epoxy and clay depend on the kind of kind of surfactant. They observed that the primary ammonium surfactants formed exfoliated nanocomposite structures while the quaternary ammonium clays formed exfoliated structures with glass epoxy. This was similarly reflected in this current work with the formation of intercalated nanocomposites.

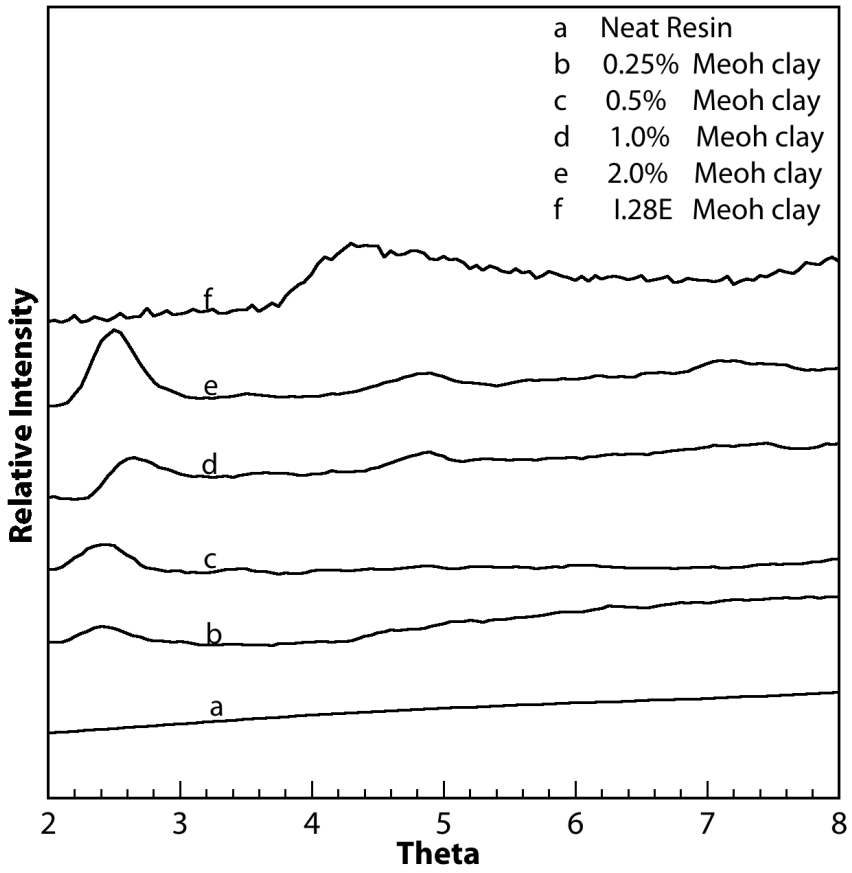

Figure 4.10: XRD curves of washed clay and their respective nanocomposites

Weight % of clay	**(2θ) (001)**	**(2θ) (002)**	**d(nm) (001)**	**d(nm) (002)**
Methanol washed clay	4.1	7.6	2.2	1.16
0.25	2.4	–	3.59	–
0.5	2.4	–	3.59	–
1.0	2.6	–	3.39	–
2.0	2.5	–	3.52	–

Table 4.4: XRD data for the methanol washed clay nanocomposites

4.4 Mechanical Characterization

Figure 4.11 shows the load displacement plots obtained during the testing of fracture specimens using single end notch beam specimens of epoxy-clay nanocomposites. The plots show the specimens having closer pre-crack length to width ratios for comparison. The neat epoxy displays a brittle failure upon reaching the critical load. However, the trend of the specimens loaded with clay was completely different. We can notice a gradual reduction in the load after reaching the peak load. The peak curves suggest toughening taking place due to addition of clay in the epoxy.

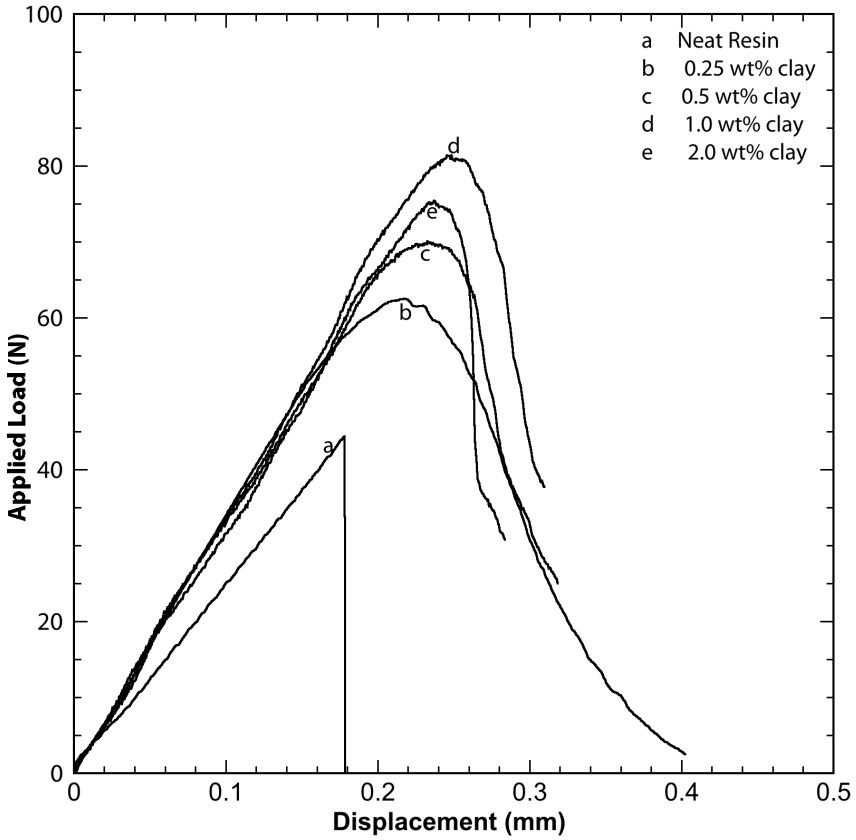

Figure 4.11: Load-Displacement plots of I.28E as-received clay-epoxy fractured specimens with varying weight % of clay in the resin

4.4.1 Fracture toughness K_{1C} of Cloisite 20A clay-epoxy nanocomposites

The specimens were loaded quasi-statically till the specimen showed a failure. The fracture toughness of the composites improved with the addition of clay. A diminutive increase in the toughness for 1.0 wt% with respect to 0.5 wt% for as-received epoxy nanocomposites, this might be due to difference in the scattering densities of clay particles in the polymer. The composite with 2.0 wt% of clay exhibited improved toughness for as-received clay. The methanol washed epoxy-clay nanocomposites also exhibited an improvement in the toughness with the addition of clay.

As-received and methanol washed clay epoxy composites displayed a similar trend in the fracture behavior for 0.25 wt% of clay loading. With further loading there was a very diminutive improvement in the fracture toughness of washed epoxy-clay nanocomposites for 1.0wt% and 2.0 wt% clay loading, as compared to as-received epoxy-clay nanocomposites. There was no substantial improvement in the toughness of the composites with washing. This suggests that in the case of Cloisite 20A epoxy nanocomposites washing of excess surfactant was not showing any effect on the fracture toughness.

4.4.2 Fracture toughness K_{1C} of Nanomer I.28E clay-epoxy nanocomposites

Figgure 4.12 shows the variation of stress intensity factor with respect to the cay weight % for I.28E clay. The curves were plotted for the as-received and washed clay nanocomposite specimens. The stress intensity of the as-received clay nanocomposites increased with addition of 1.0 wt% of clay and reduced with further addition of 2.0 wt% of clay. The reduction in the toughness was attributed to the formation of clay aggregates which acts as areas of stress concentration and reduces the properties.

The epoxy composites made with washed clay showed a similar trend in the fracture behavior. The toughness was improved with the addition of clay. The composites having 0.5 wt%, 1.0 wt% and 2.0 wt% displayed similar fracture toughness. The reason for no greater improvement in the toughness for 0.5 wt%, 1.0 wt% and 2.0 wt% loaded nanocom-

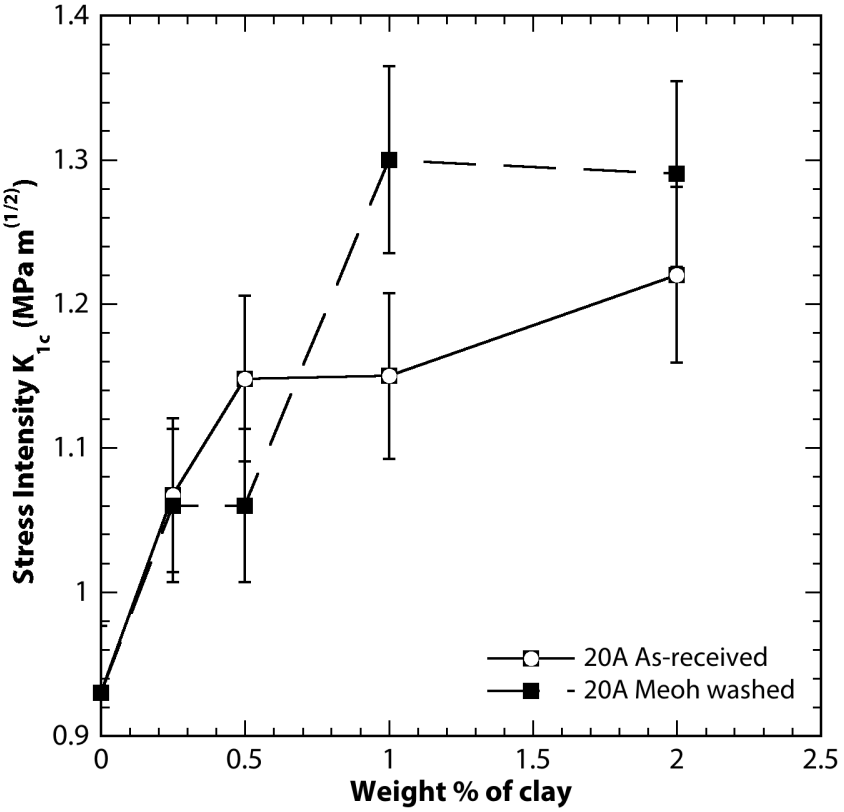

Figure 4.12: Fracture toughness of as-received and washed clay

posites was due to the agglomerates formed during the mixing process. Looking into the plots with error bars, we can conclude that clay washing did not greatly change the fracture properties of the epoxy composites reinforced with 28E washed clay.

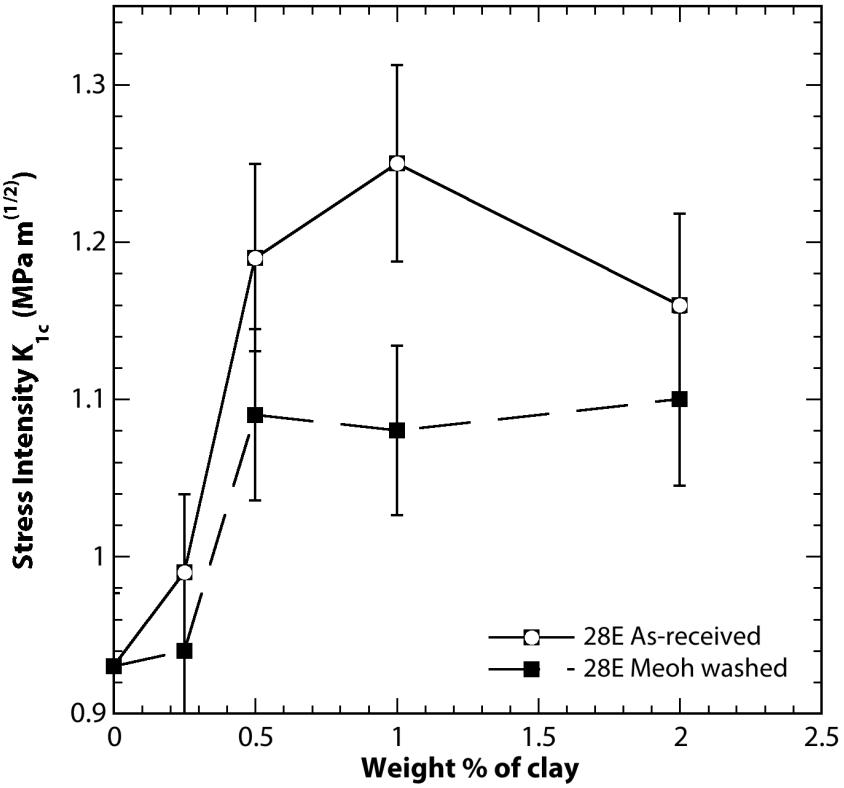

Figure 4.13: Fracture toughness of as-received and washed clay

4.4.3 Flexure testing of Cloisite 20A clay-epoxy nanocomposites

Figure 4.13 shown below was plotted for the weight % of clay and flexure modulus of as-received and washed clay epoxy nanocomposites. There was an improvement in the modulus with increased clay loading till 1.0 wt% and a reduction in the modulus was noticed with the further addition of 2.0 wt% of as-received clay. This was due to the formation of isolated clay aggregates. The difference between the modulus of the as-received and washed samples were diminutive and no substantial variation can be observed due to the large scatter of data. A similar behavior in tensile modulus was observed for the composites

made of as-received and washed clays by Cui $et.\ al.$ [48]. The plot 4.14 shows the data of

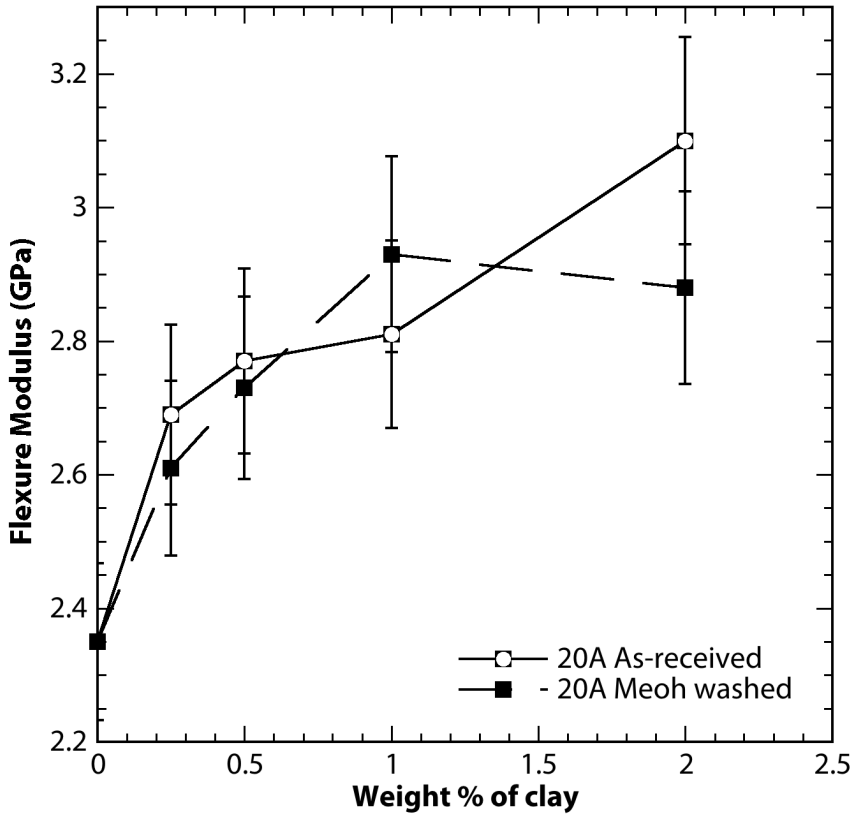

Figure 4.14: Modulus of as-received and washed clay

flexural strength for unwashed and washed clays. The strength of the both clays remained almost similar to each other.

4.4.4 Flexure testing of Nanomer I.28E epoxy-clay nanocomposites

The graph 4.15 shows the trend for the variation of flexure modulus of as-received and washed clay reinforced composites. The samples displayed an improvement in the modulus for increasing clay content till 1.0wt% and no further improvement in the modulus was found for 2.0 wt% clay loaded epoxy nanocomposites.

With the incorporation of washed clay in epoxy resin a slight or diminutive reduction in the toughness was observed for 1.0 wt% and 2.0 wt% clay (both remained almost

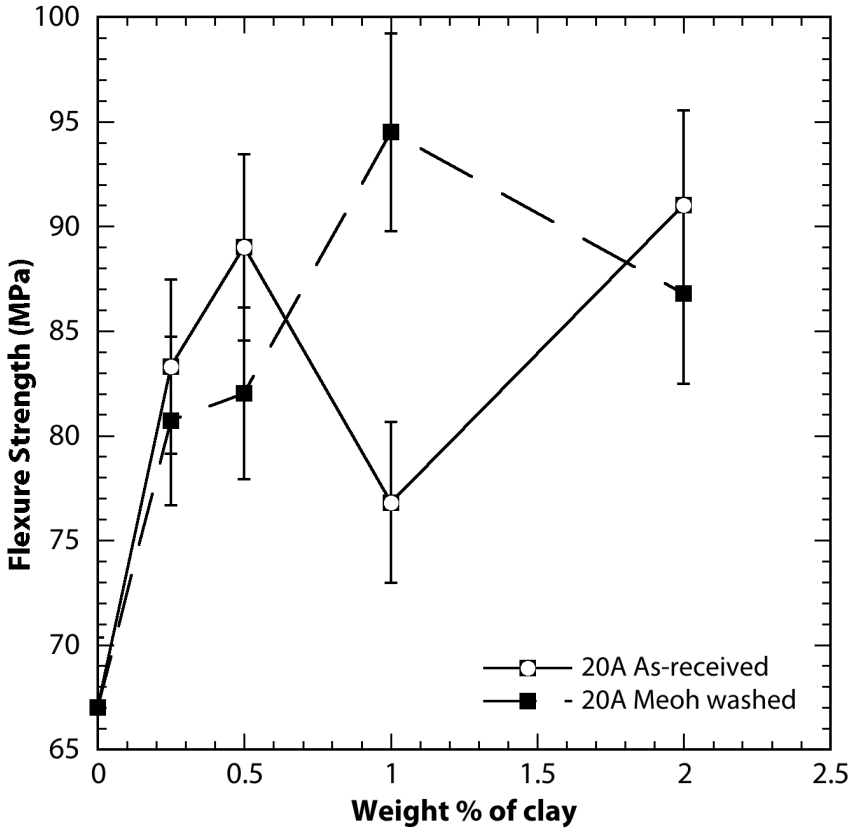

Figure 4.15: Strength of as-received and washed clay

similar) loaded epoxy composites with respect to the as-received epoxy-clay nanocomposites. Figure. 4.17 shows the relation between weight % of clay and flexure strength

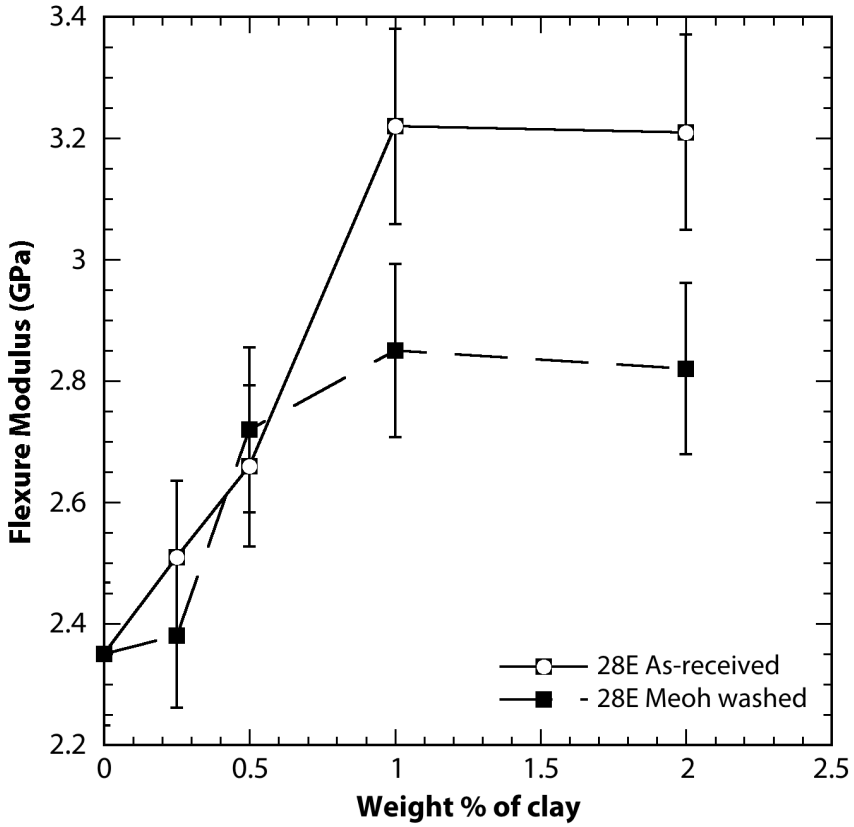

Figure 4.16: Modulus of as-received and washed clay

of the nanocomposite. The strength of the composite increased with the incorporation of the washed clays till 1.0 wt% and reduced due to agglomeration with further addition of clay (as per the XRD data). The as-received clay nanocomposites displayed a reduction in the strength for 0.25 wt% and 0.5wt% loaded nanocomposite while an improvement was noticed for the 2.0wt% clay. This variation was again diminutive.

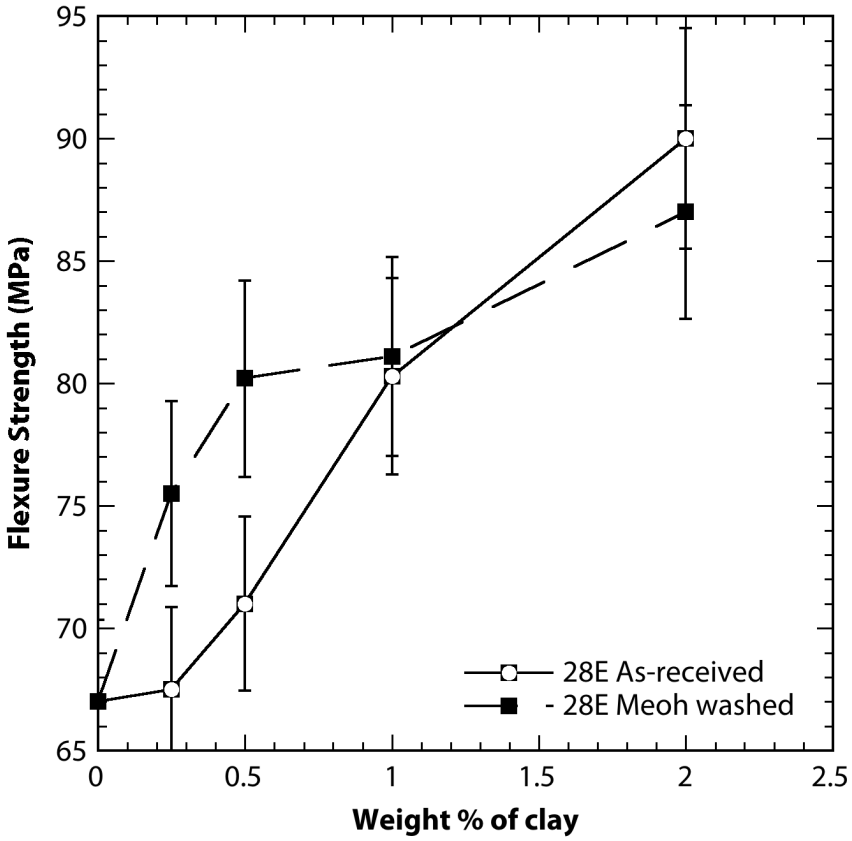

Figure 4.17: Strength of as-received and washed clay

4.5 Scanning Electron Microscopy

4.5.1 Fracture morphology of Cloisite 20A clay and their epoxy nanocomposites

The scanning electron microscopy was carried to study the morphology of the fractured specimens. Nanocomposites fabricated with as-received clay were studied. The fig. 4.18 a. b. shows the image of a neat epoxy sample with a brittle failure at the surface. The fig. 4.18 a. shows the starter crack zone and the beginning of delamination zone. The fig. b. shows the image of the center portion of crack. This displayed a wave pattern which was due to the stress waves which were generated due to the catastrophic failure due to the brittle failure of the sample.

The image 4.19 a. displays the surface of the starter crack and the begining of the failure zone. The area with the starter crack shows a smooth surface followed by a region with very few rough markings due to the crack bridging by the clay particles. The image 4.19 b. shows the surface of the sample at a distance from the starter crack (mid portion of the crack). There were increased rivermarkings observed which explains that the clay helped in improving the toughness of the specimen.

Fig. 4.20 a. shows the failure of 1.0 wt% clay epoxy nanocomposite with a starter crack. When taken a look at the beginning of the delamination zone, the surface roughness of the sample was observed. This explains the increased % of clay was preventing the crack to penetrate through it. Fig. 4.20 b. the fractured surface with increased clay loading of 1.0 weight % displayed an improvement in the toughness. The river-line markings and the more zigzag path of the cracks shows a very good interaction of clay with the polymer. The semi-circles in the failure regions shows the way the crack was stopped by the clay platelets. This was the crack pinning mechanism exhibited by the clay in the composites.

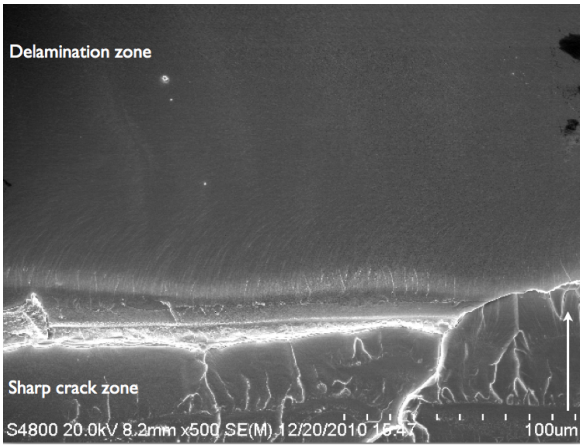

(a) fracture image showing the starter crack and the initiation of fracture region

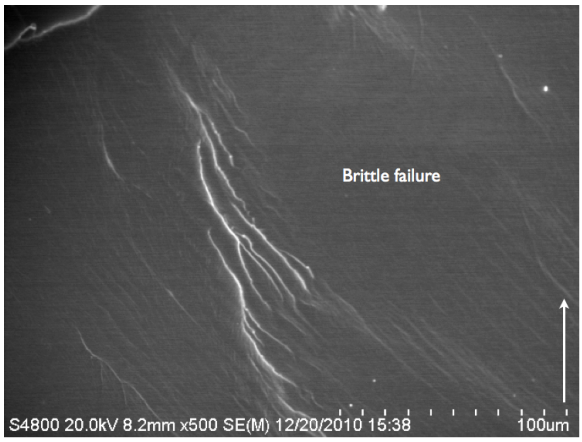

(b) fracture image showing the brittle region with stress waves

Figure 4.18: Epon 862 neat resin fracture specimen

The fracture morphology of the nanocomposites made of methanol washed clay were discussed. The nanocomposites with 0.25 wt % methanol washed clay showed a similar kind of behavior like 0.25wt% as-received clay nanocomposites. Fig. 4.21 a. displays the morphology of the crack front beginning with a starter crack followed by more surface roughness.

Fig. 4.21 b. shows the morphology of the fractured sample with more microcracks in the central region of the failed specimen which was also similar to the as-received clay nanocomposites.

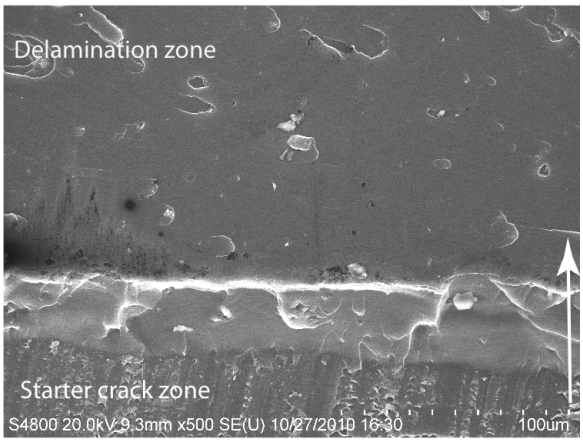

(a) fracture image showing the starter crack and the initiation of fracture region

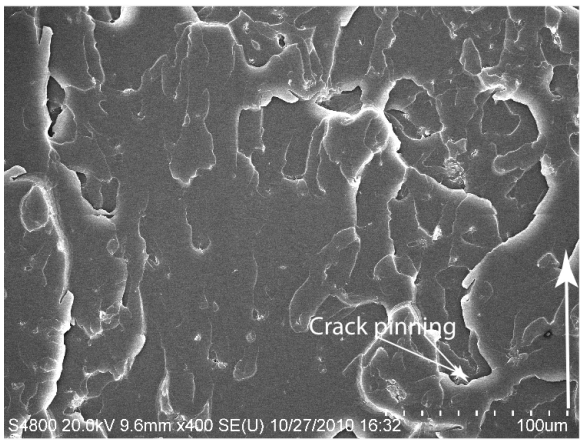

(b) fracture image showing the roughened region

Figure 4.19: Epon 862/20A having 0.25 wt% of as-received clay

4.5.2 Fracture morphology of Nanomer I.28E clay and their epoxy nanocomposites

Figure. 4.18a. b. shows the SEM micrograph of the neat resin sample showing a brittle failure. Figure. 4.22 a. shows the region of starter crack and the crack delamination zone for the nanocomposites with 0.25wt% of as-received clay. The following micrograph 4.22 b. shows the surface morphology of the fractured specimen at the center portion of the crack. There were few rivermarkings on the surface indicating less resistance offered for the crack to propagation. There was no subcritical crack growth region observed indicating

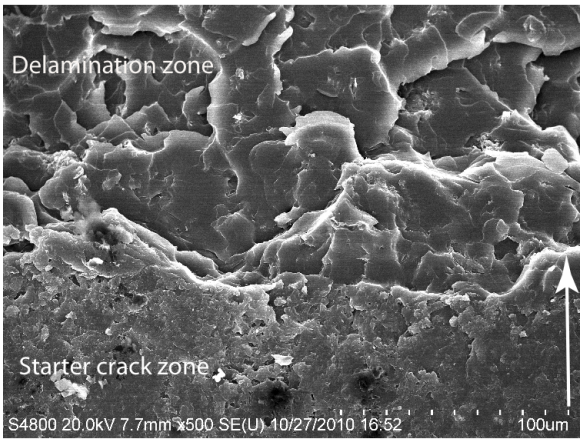

(a) fracture image showing the starter crack and the initiation of fracture region

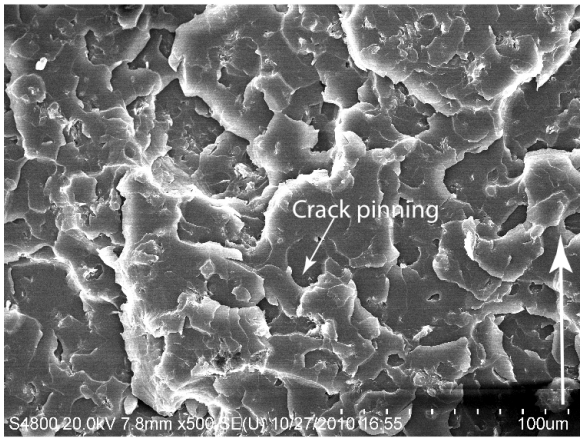

(b) fracture image showing the roughened region

Figure 4.20: Epon 862/20A having 1.0 wt% of as-received clay

no extreme toughening taking place.

The micrographs 4.23 a. and 4.23 b. shows the morphology of the 2 wt% as-received clay reinforced epoxy fractured samples. The image 4.23 a. shows the starter crack and the initiation of the crack front. The beginning of the crack tip was not very rough, but when the center portion of the crack was observed the roughness gradually increased. Fig. 4.23 b. explains extrinsic toughening taking place on the surface. The micro cracks were more in number compared to the 0.25 wt% clay composite. The number of microcracks were grown in number indicating the increase in the resistance for crack growth which obviously

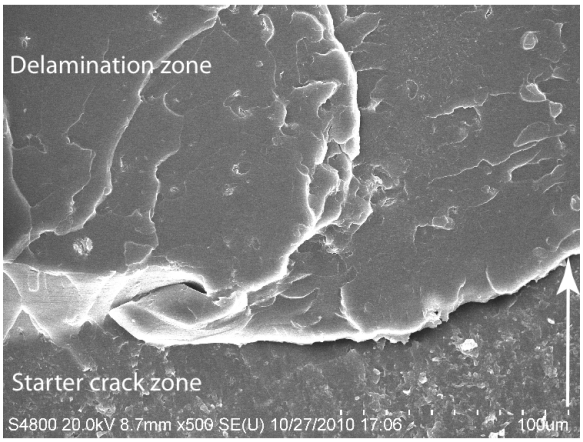

(a) fracture image showing the starter crack and the initiation of fracture region

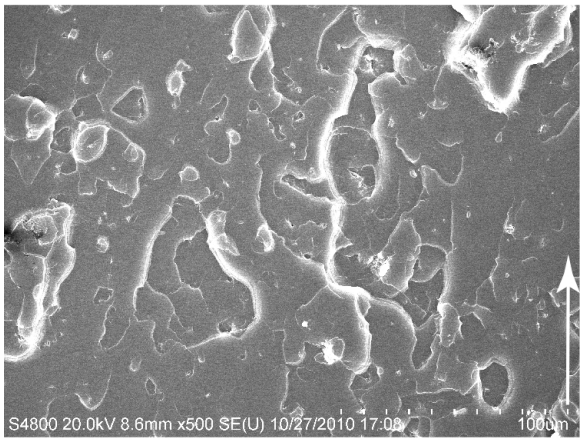

(b) fracture image showing the roughened region

Figure 4.21: Epon 862/20A having 0.25wt% of methanol washed clay

improves the toughness.

Small regions on the image could be spotted which can be anticipated to be the aggregates which were generated due to the differences in the scattering densities of the clay and epoxy during the mixing process.

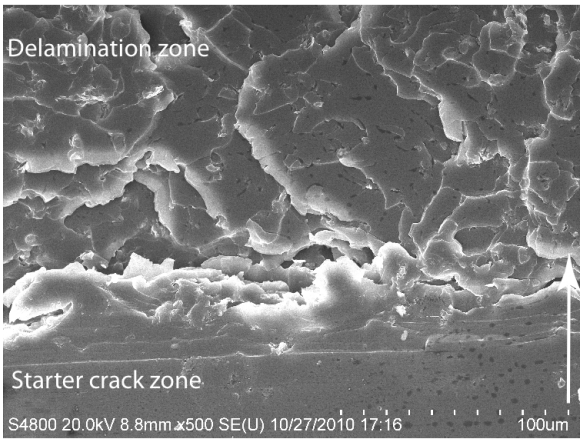

(a) fracture image showing the starter crack and the initiation of fracture region

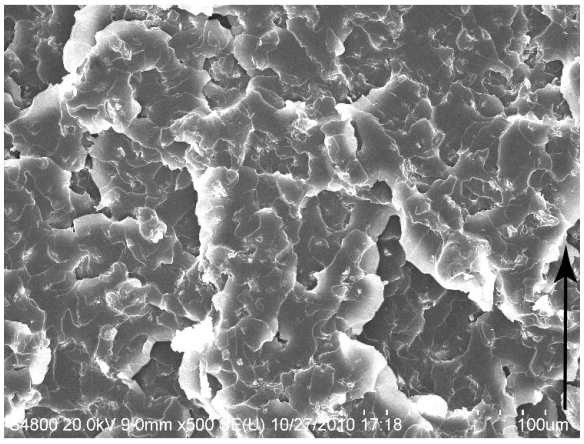

(b) fracture image showing the roughened region

Figure 4.22: Epon 862/20A having1.0wt% of methanol washed clay

The SEM images 4.24 a. and 4.24 b. exhibits the failure surface of the epoxy samples reinforced with 0.25 wt% methanol washed clay. The image a. has the starter crack with low amount of cracks on the surface. When looked further into the fracture surface of the specimen we can notice roughened regions with big particles aggregates which acts as areas of stress concentration and reduced the strength of the composite at higher loadings rates. When an applied stress reaches these large aggregates, there will be generation of localized stresses making the specimen to fail catastrophically.

The micrographs display the fracture images of the 2.0 wt% washed clay specimens.

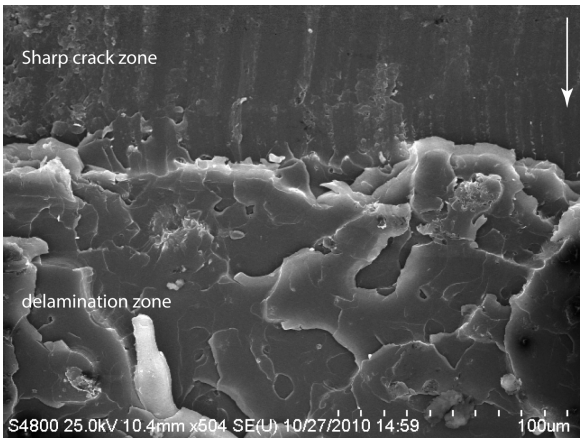

(a) fracture image showing the starter crack and the initiation of fracture region

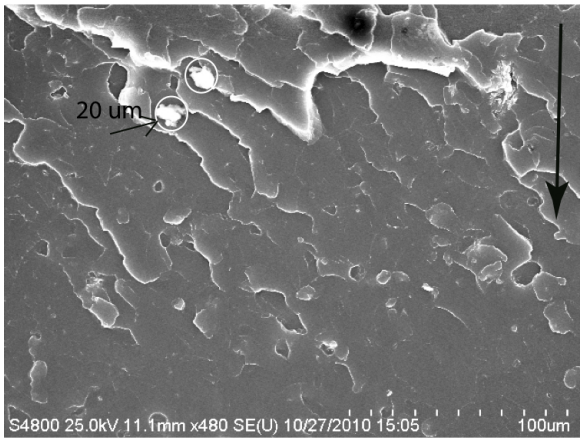

(b) fracture image showing the roughened region

Figure 4.23: Epon 862/28E having 0.25 wt% of as-received clay

The images shows a rough portion indicating a higher clay loading. Fig. 4.25 b. shows the SEM image with clay agglomerates which are more in number which might have caused reduced fracture toughness.

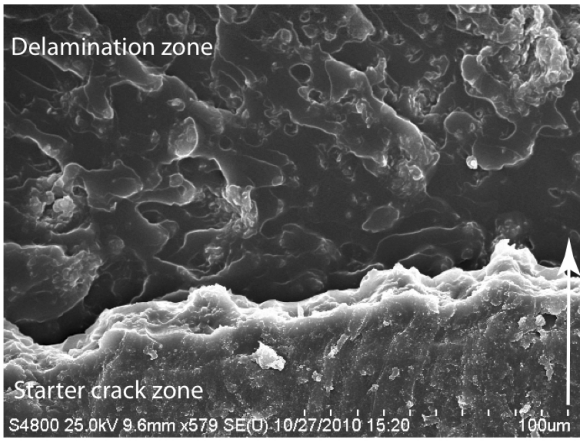

(a) fracture image showing the starter crack and the initiation of fracture region

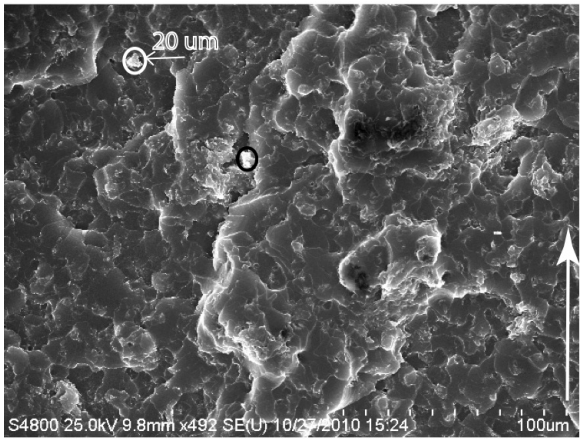

(b) fracture image showing the roughened region

Figure 4.24: Epon 862/28E having 2.0 wt% of as-received clay

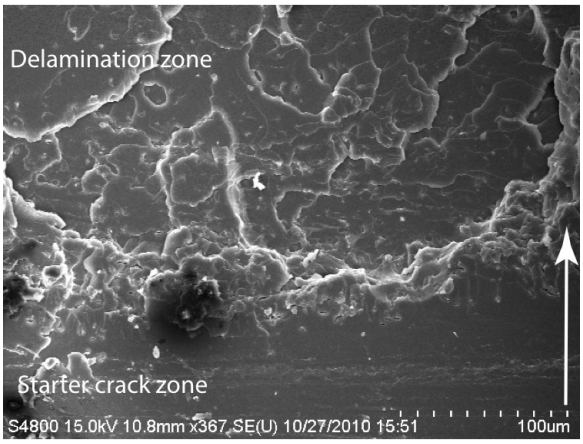

(a) fracture image showing the starter crack and the initiation of fracture region

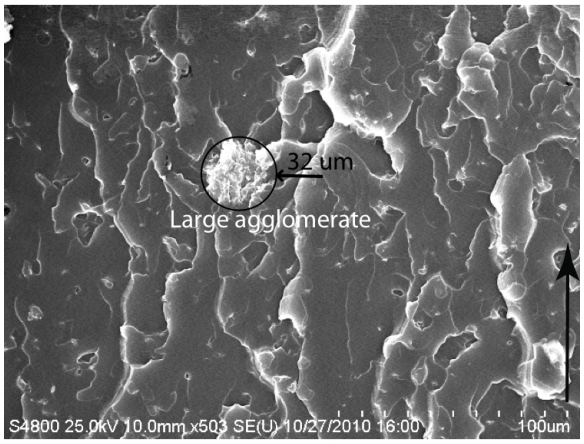

(b) fracture image showing the roughened region

Figure 4.25: Epon 862/28E having 0.25 wt% of methanol washed clay

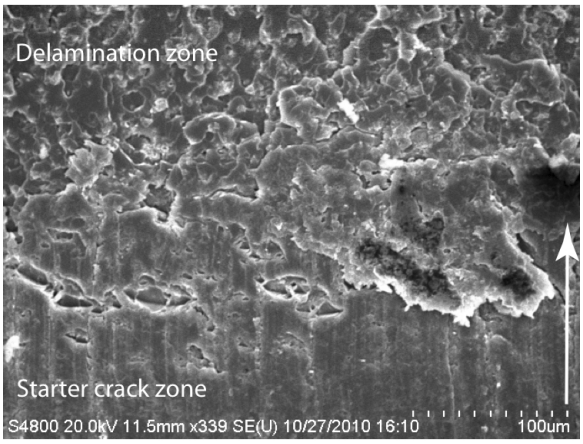

(a) fracture image showing the starter crack and the initiation of fracture region

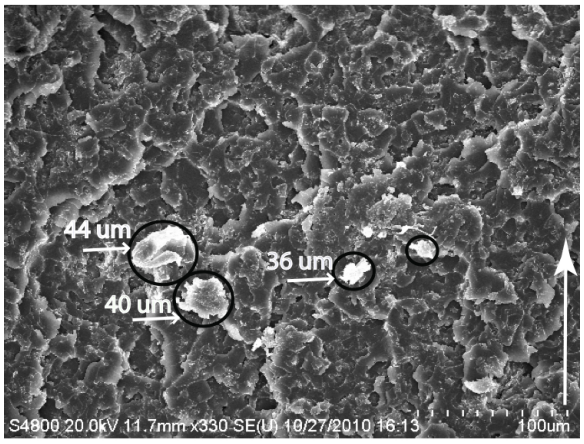

(b) fracture image showing the roughened region

Figure 4.26: Epon 862/28E having 2.0 wt% of methanol washed clay

CHAPTER 5

CONCLUSION and FUTURE WORK

As-received and washed clays with their corresponding nanocomposites were subjected to thermal degradation. Mechanical properties like fracture toughness, flexure modulus were measured and the fractured sample's morphology was studied using SEM imaging. The silver nitrate test confirmed the loss of surfactant molecules from the organoclays through washing. The washed clays displayed a variation in degradation profiles with a shift to the higher temperature region in the graph. An improvement in the onset of degradation temperature and thermal stability for both the organoclays was found. Their corresponding nanocomposites did not show any improvement in the onset of decomposition temperature but the thermal stability of the composites was slightly improved.

Fracture toughness for the Cloisite 20A methanol washed epoxy nanocomposites showed a very slight improvement upon washing which was negligible. The flexure modulus remained insignificant. Similarly, I.28E displayed the same behavior in terms of fracture toughness and flexure modulus. The methanol washed organoclays displayed an improvement in the thermal degradation temperature indicating removal of surfactant. The nanocomposites made out of this washed clay did not show any substantial variation in the thermal degradation patterns. SEM imaging helped in understanding the morphology of the specimens. Aggregates were found for the composites fabricated with I.28 E clay. This indicated that removal of excess surfactant from the clay galleries did not show any substantial or quantifiable variation on the mechanical as-well as thermal properties of epoxy-clay reinforced composites. It was understood that removal of excess surfactant did not have any impact on the mechanical and thermal properties of epoxy-clay nanocomposites.

It will be worthy to incorporate and study the effect of the washing on the mechanical and thermal properties of phosphonium modified clay and transition metal ion (TMI) modified clays in epoxy resins due to their high thermal stability. Industries will be benefitted if they can incorporate high temperature with standing clays in the resins and study their mechanical properties for high performance, where TMI's and phosphonium modified clays will be the suitable clays which will be the future work.

BIBLIOGRAPHY

[1] D. R. Paul and L. M. Robeson, "Polymer nanotechnology: Nanocomposites," *POLYMER*, vol. 49, pp. 3187–3204, JUL 7 2008.

[2] Z. Zhao, F. Liu, L. Zhao, and S. Yan, "XPS study on BiI3-nylon 11 nanocomposites," *MATERIALS CHEMISTRY AND PHYSICS*, vol. 124, pp. 55–59, NOV 1 2010.

[3] B. Y. Yeom, E. Shim, and B. Pourdeyhimi, "Boehmite nanoparticles incorporated electrospun nylon-6 nanofiber web for new electret filter media," *MACROMOLECULAR RESEARCH*, vol. 18, pp. 884–890, SEP 2010.

[4] L. Cui and J.-T. Yeh, "Nylon 6 Crystal-Phase Transition in Nylon 6/Clay/Poly(vinyl alcohol) Nanocomposites," *JOURNAL OF APPLIED POLYMER SCIENCE*, vol. 118, pp. 1683–1690, NOV 5 2010.

[5] Y. J. Kim and K. A. Harries, "Modeling of timber beams strengthened with various CFRP composites," *ENGINEERING STRUCTURES*, vol. 32, pp. 3225–3234, OCT 2010.

[6] W. Z. Nie, X. Z. Li, and Y. H. Su, "Effect of Carbon Fiber Surface Oxidation on Tribological Properties of PTFE Composite under Oil-Lubricated Conditions," *COMPOSITE INTERFACES*, vol. 17, no. 4, pp. 337–346, 2010.

[7] M. Haendel, D. Nickel, G. Alisch, and T. Lampke, "Hard anodizing of a coarse and an ultrafine-grained aluminium-copper alloy with incorporated alumina and silicon carbide particles," *MATERIALWISSENSCHAFT UND WERKSTOFFTECHNIK*, vol. 41, pp. 737–743, SEP 2010.

[8] M. Jayasankar, K. P. Hima, S. Ananthakumar, P. Mukundan, P. K. Pillai, and K. G. K. Warrier, "Role of particle size of alumina on the formation of aluminium titanate as well as on sintering and microstructure development in sol-gel alumina-aluminium titanate composites," *MATERIALS CHEMISTRY AND PHYSICS*, vol. 124, pp. 92–96, NOV 1 2010.

[9] G. Roudini, R. Tavangar, L. Weber, and A. Mortensen, "Influence of reinforcement contiguity on the thermal expansion of alumina particle reinforced aluminium composites," *INTERNATIONAL JOURNAL OF MATERIALS RESEARCH*, vol. 101, pp. 1113–1120, SEP 2010.

[10] A. L. Sharma and A. K. Thakur, "Improvement in Voltage, Thermal, Mechanical Stability and Ion Transport Properties in Polymer-Clay Nanocomposites," *JOURNAL OF APPLIED POLYMER SCIENCE*, vol. 118, pp. 2743–2753, DEC 5 2010.

[11] G. Leone, A. Boglia, F. Bertini, M. Canetti, and G. Ricci, "Designed Organo-Layered Silicates as Nanoreactors for 1,3-Butadiene Stereospecific Polymerization Toward Rubber Nanocomposites Synthesis," *JOURNAL OF POLYMER SCIENCE PART A-POLYMER CHEMISTRY*, vol. 48, pp. 4473–4483, SEP 15 2010.

[12] J. M. Herrera-Alonso, Z. Sedlakova, and E. Marand, "Gas transport properties of polyacrylate/clay nanocomposites prepared via emulsion polymerization," *JOURNAL OF MEMBRANE SCIENCE*, vol. 363, pp. 48–56, NOV 1 2010.

[13] O. I. H. Dimitry, Z. I. Abdeen, E. A. Ismail, and A. L. G. Saad, "Preparation and properties of elastomeric polyurethane/organically modified montmorillonite nanocomposites," *JOURNAL OF POLYMER RESEARCH*, vol. 17, pp. 801–813, NOV 2010.

[14] S. Utzschneider, F. Becker, T. M. Grupp, B. Sievers, A. Paulus, O. Gottschalk, and V. Jansson, "Inflammatory response against different carbon fiber-reinforced PEEK

wear particles compared with UHMWPE in vivo," *ACTA BIOMATERIALIA*, vol. 6, pp. 4296–4304, NOV 2010.

[15] S. P. Sharma and S. C. Lakkad, "Compressive strength of carbon nanotubes grown on carbon fiber reinforced epoxy matrix multi-scale hybrid composites," *SURFACE & COATINGS TECHNOLOGY*, vol. 205, pp. 350–355, OCT 15 2010.

[16] E. S. Cozza, O. Monticelli, and E. Marsano, "Electrospinning: A Novel Method to Incorporate POSS Into a Polymer Matrix," *MACROMOLECULAR MATERIALS AND ENGINEERING*, vol. 295, pp. 791–795, SEP 14 2010.

[17] M. Sanchez-Soto, S. Illescas, H. Milliman, D. A. Schiraldi, and A. Arostegui, "Morphology and Thermomechanical Properties of Melt-Mixed Polyoxymethylene/Polyhedral Oligomeric Silsesquioxane Nanocomposites," *MACROMOLECULAR MATERIALS AND ENGINEERING*, vol. 295, pp. 846–858, SEP 14 2010.

[18] J.-H. Jeon, J.-H. Lim, and K.-M. Kim, "Organic-Inorganic Hybrid Nanocomposites of Poly(sodium 4-styrenesulfonate) and Octafunctional Polyhedral Oligomeric Silsesquioxane (POSS)," *MACROMOLECULAR RESEARCH*, vol. 18, pp. 341–345, APR 2010.

[19] J. Xu, P. Yao, L. Liu, Z. Jiang, F. He, M. Li, and J. Zou, "Synthesis and Characterization of an Organic Soluble and Conducting Polyaniline-Grafted Multiwalled Carbon Nanotube Core-Shell Nanocomposites by Emulsion Polymerization," *JOURNAL OF APPLIED POLYMER SCIENCE*, vol. 118, pp. 2582–2591, DEC 5 2010.

[20] S. Kalmodia, S. Goenka, T. Laha, D. Lahiri, B. Basu, and K. Balani, "Microstructure, mechanical properties, and in vitro biocompatibility of spark plasma sintered hydroxyapatite-aluminum oxide-carbon nanotube composite," *MATERIALS SCIENCE & ENGINEERING C-MATERIALS FOR BIOLOGICAL APPLICATIONS*, vol. 30, pp. 1162–1169, OCT 12 2010.

[21] S. Santangelo, G. Messina, G. Faggio, A. Donato, L. De Luca, N. Donato, A. Bonavita, and G. Neri, "Micro-Raman analysis of titanium oxide/carbon nanotubes-based nanocomposites for hydrogen sensing applications," *JOURNAL OF SOLID STATE CHEMISTRY*, vol. 183, pp. 2451–2455, OCT 2010.

[22] V. Ijeri, L. Cappelletto, S. Bianco, M. Tortello, P. Spinelli, and E. Tresso, "Nafion and carbon nanotube nanocomposites for mixed proton and electron conduction," *JOURNAL OF MEMBRANE SCIENCE*, vol. 363, pp. 265–270, NOV 1 2010.

[23] H. Ha, S. C. Kim, and K. Ha, "Morphology and Properties of Polyamide/Multi-walled Carbon Nanotube Composites," *MACROMOLECULAR RESEARCH*, vol. 18, pp. 660–667, JUL 2010.

[24] J. Lee, D. R. Hwang, J. Hong, D. Jung, and S. E. Shim, "Significance of the Dispersion Stability of Carbon Nanotubes on the Thermal Conductivity of Nylon 610 Nanocomposite," *JOURNAL OF DISPERSION SCIENCE AND TECHNOLOGY*, vol. 31, no. 9, pp. 1230–1235, 2010.

[25] M. Pan, S. Xing, J. Yuan, J. Wu, and L. Zhang, "Synthesis and Characterization of Poly(butyl acrylate-co-ethylhexyl acrylate)/Poly(vinyl chloride)[P(BA-EHA)/PVC] Novel Core-Shell Modifier and Its Impact Modification for a Poly(vinyl chloride)-Based Blend," *POLYMER ENGINEERING AND SCIENCE*, vol. 50, pp. 1085–1094, JUN 2010.

[26] Q. Zhang, Q. Liu, J. E. Mark, and I. Noda, "A novel biodegradable nanocomposite based on poly (3-hydroxybutyrate-co-3-hydroxyhexanoate) and silylated kaolinite/silica core-shell nanoparticles," *APPLIED CLAY SCIENCE*, vol. 46, pp. 51–56, SEP 2009.

[27] R. Vaia and E. Giannelis, "Polymer nanocomposites: Status and opportunities," *MRS BULLETIN*, vol. 26, pp. 394–401, MAY 2001.

[28] Y. KOJIMA, M. USUKI A, KAWASUMI, A. OKADA, Y. FUKUSHIMA, T. KURAUCHI, and K. O, "MECHANICAL-PROPERTIES OF NYLON 6-CLAY HYBRID," *JOURNAL OF MATERIALS RESEARCH*, vol. 8, pp. 1185–1189, MAY 1993.

[29] A. Leite, L. Maia, O. Pereira, E. Araujo, H. Lira, and W. de Castro, "MECHANICAL PROPERTIES OF NYLON6/BRAZILIAN CLAY NANOCOMPOSITES," *JOURNAL OF ALLOYS AND COMPOUNDS*, vol. 495, no. 2, pp. 596–597, 2010.

[30] J. Weon and H. Sue, "EFFECTS OF CLAY ORIENTATION AND ASPECT RATIO ON MECHANICAL BEHAVIOR OF NYLON-6 NANOCOMPOSITES," *POLYMER SCIENCE*, vol. 46, no. 17, pp. 6325–6334, 2005.

[31] B. Han, G. Ji, and J. Wu, SS andShen, "PREPARATION AND CHARACTERIZATION OF NYLO 66/MONTMORILLONITE NANOCOMPOSITES WITH CO-TREATED MONTMORILLONITES," *EUROPEAN POLYMER JOURNAL*, vol. 39, no. 8, pp. 1641–1646, 2003.

[32] M. Lai and J.-K. Kim, "EFFECTS OF EPOXY TREATMENT OF ORGANOCLAY ON STRUCTURE, THERMO-MECHANICAL AND TRANSPORT PROPERTIES OF POLY(EHTYLENE TEREPTHALATE-CO- APTHALATE)/ORGANOCLAY NANOCOMPOSITES ," *POLYMER SCIENCE*, vol. 46, no. 13, pp. 4722–4734, 2005.

[33] D. Shah, RK andPaul, "NYLON-6 NANOCOMPOSITES PREPARED BY A MELT MIXIN MASTERBATCH PROCESS," *POLYMER SCIENCE*, vol. 45, no. 9, pp. 2991–3000, 2004.

[34] N. A. Siddiqui, R. S. C. Woo, J.-K. Kim, C. C. K. Leung, and A. Munir, "Mode I interlaminar fracture behavior and mechanical properties of CFRPs with nanoclay-filled epoxy matrix," *COMPOSITES PART A-APPLIED SCIENCE AND MANUFACTURING*, vol. 38, no. 2, pp. 449–460, 2007.

[35] A. Yasmin, J. J. Luo, J. L. Abot, and I. M. Daniel, "Mechanical and thermal behavior of clay/epoxy nanocomposites," *COMPOSITES SCIENCE AND TECHNOLOGY*, vol. 66, pp. 2415–2422, NOV 2006.

[36] J. Wang and S. Qin, "Study on the thermal and mechanical properties of epoxy-nanoclay composites: The effect of ultrasonic stirring time," *MATERIALS LETTERS*, vol. 61, pp. 4222–4224, AUG 2007.

[37] S. Zunjarrao, R. Sriraman, and R. Singh, "Effect of processing parameters and clay volume fraction on the mechanical properties of epoxy-clay nanocomposites," *JOURNAL OF MATERIALS SCIENCE*, vol. 41, pp. 2219–2228, APR 2006.

[38] A. Jandro, L, Y. Asma, and D. Issac, M, "MECHANICAL AND THERMOVISCOELASTIC BEHAVIOR OF CLAY/EPOXY NANOCOMPOSITES," *MATERIALS RESERACH SOCIETY SYMPOSIUM PROCEEDINGS 740*, 2003.

[39] W. P. Liu, S. V. Hoa, and M. Pugh, "Fracture toughness and water uptake of high-performance epoxy/nanoclay nanocomposites," *COMPOSITES SCIENCE AND TECHNOLOGY*, vol. 65, pp. 2364–2373, DEC 2005.

[40] S. Zainuddin, M. V. Hosur, Y. Zhou, A. Kumar, and S. Jeelani, "Durability studies of montmorillonite clay filled epoxy composites under different environmental conditions," *MATERIALS SCIENCE AND ENGINEERING A-STRUCTURAL MATERIALS PROPERTIES MICROSTRUCTURE AND PROCESSING*, vol. 507, pp. 117–123, MAY 15 2009.

[41] S. K. Sharma and S. K. Nayak, "Surface modified clay/polypropylene (PP) nanocomposites: Effect on physico-mechanical, thermal and morphological properties," *POLYMER DEGRADATION AND STABILITY*, vol. 94, pp. 132–138, JAN 2009.

[42] T. D. Ngo, M. T. Ton-That, S. V. Hoa, and K. C. Cole, "Effect of temperature, duration and speed of pre-mixing on the dispersion of clay/epoxy nanocomposites ," *Composites Science and Technology*, vol. 69, pp. 1831–1840, 9 April 2009.

[43] H. A. Patel, R. S. Somani, H. C. Bajaj, and R. V. Jasra, "Preparation and characterization of phosphonium montmorillonite with enhanced thermal stability," *APPLIED CLAY SCIENCE*, vol. 35, pp. 194–200, FEB 2007.

[44] J. U. Calderon, B. Lennox, and M. R. Kamal, "Thermally stable phosphonium-montmorillonite organoclays," *APPLIED CLAY SCIENCE*, vol. 40, pp. 90–98, JUN 2008.

[45] L. Cui, D. M. Khrarnov, C. W. Bielawski, D. L. Hunter, P. J. Yoon, and D. R. Paul, "Effect of organoclay purity and degradation on nanocomposite performance, Part 1: Surfactant degradation," *POLYMER*, vol. 49, pp. 3751–3761, AUG 11 2008.

[46] C. B. Hedley, G. Yuan, and B. K. G. Theng, "Thermal analysis of montmorillonites modified with quaternary phosphonium and ammonium surfactants," *APPLIED CLAY SCIENCE*, vol. 35, pp. 180–188, FEB 2007.

[47] J. Li and J. P. Oberhauser, "The effect of free surfactant and grafted surfactant surface coverage on the rheology of organoclay dispersions," *JOURNAL OF RHEOLOGY*, vol. 50, pp. 729–747, SEP-OCT 2006.

[48] L. Cui, D. L. Hunter, P. J. Ybon, and D. R. Paul, "Effect of organoclay purity and degradation on nanocomposite performance, Part 2: Morphology and properties of nanocomposites," *POLYMER*, vol. 49, pp. 3762–3769, AUG 11 2008.

[49] A. Morgan and J. Harris, "Effects of organoclay Soxhlet extraction on mechanical properties, flammability properties and organoclay dispersion of polypropylene nanocomposites," *POLYMER*, vol. 44, pp. 2313–2320, APR 2003.

[50] P. Nawani, M. Y. Gelfer, B. S. Hsiao, A. Frenkel, J. W. Gilman, and S. Khalid, "Surface modification of nanoclays by catalytically active transition metal ions," *LANGMUIR*, vol. 23, pp. 9808–9815, SEP 11 2007.

[51] J. Park and S. Jana, "Adverse effects of thermal dissociation of alkyl ammonium ions on nanoclay exfoliation in epoxy-clay systems," *POLYMER*, vol. 45, pp. 7673–7679, OCT 13 2004.

[52] F. Carrasco and P. Pages, "Thermal degradation and stability of epoxy nanocomposites: Influence of montmorillonite content and cure temperature," *POLYMER DEGRADATION AND STABILITY*, vol. 93, pp. 1000–1007, MAY 2008.

[53] P. I. Xidas and K. S. Triantafyllidis, "Effect of the type of alkylammonium ion clay modifier on the structure and thermal/mechanical properties of glassy and rubbery epoxy-clay nanocomposites," *EUROPEAN POLYMER JOURNAL*, vol. 46, pp. 404–417, MAR 2010.

[54] G. LAGALY and R. MALBERG, "DISAGGREGATION OF ALKYLAMMONIUM MONTMORILLONITES IN ORGANIC-SOLVENTS," *COLLOIDS AND SURFACES*, vol. 49, pp. 11–27, OCT 15 1990.

[55] N. Tran, G. Dennis, A. Milev, G. Kannangara, P. Williams, M. Wilson, and R. Lamb, "Dispersion of organically modified clays within n-alcohols," *JOURNAL OF COLLOID AND INTERFACE SCIENCE*, vol. 297, pp. 541–545, MAY 15 2006.

[56] American, Society, of Testing, and Materials, "Standard test methods for Plane Strain fracture toughness and Strain Energy Release Rate for Plastic Materials," *Annual book of ASTM standards Designation D5045*, 1999.

[57] American, Society, of Testing, and Materials, "Standard test methods for Flexure Properties of Unreinforced and Reinforced Plastics and Electrical Insulating Materials," *Annual book of ASTM standards Designation D790 07*, 1999.

VITA

Chaitanya V. Viswanadha

Candidate for the Degree of

Master of Science

Thesis: THE EFFECT OF EXCESS SURFACTANT REMOVAL ON THE THERMO-MECHANICAL BEHAVIOR OF EPOXY-CLAY NANOCOMPOSITES

Major Field: Mechanical and Aerospace Engineering (Solid Mechanics & Design)

Biographical:

Personal Data: Born in Hyderabad, Andhra Pradesh, India, on July 2nd, 1986.

Education:

Received the Bachelors degree from Jawaharlal Nehru Technological University, Hyderabad, Andhra Pradesh, India, 2008, in Mechanical Engineering.
Completed the requirements for the degree of Master of Science with a major in Mechanical Engineering, Oklahoma State University in May, 2011.

Experience:

Worked as a Graduate Research Assistant at the Mechanics of Advanced Materials Laboratory led by Dr. Raman P. Singh in the field of nanoclay reinforced polymer composites.
Worked as a Graduate Teaching Assistant in Mechanical and Aerospace Engineering department at Oklahoma State University, Stillwater, USA, January 2009–May 2010

Name: Chaitanya V. Viswanadha Date of Degree: May, 2011

Institution: Oklahoma State University Location: Stillwater, Oklahoma

Title of Study: THE EFFECT OF EXCESS SURFACTANT REMOVAL ON THE THERMO-MECHANICAL BEHAVIOR OF EPOXY-CLAY NANOCOMPOSITES

Pages in Study: 61 Candidate for the Degree of Master of Science

Major Field: Mechanical and Aerospace Engineering (Solid Mechanics & Design)

This study investigates the resultant thermal and mechanical properties of epoxy composites reinforced with as-received and washed (clay with excess surfactant removed) organoclay. Two commercially available organoclays: Cloisite 20A (modified with dimethyl dihydrogenated tallow quaternary ammonium salt) and Nanomer I.28E (modified with quaternary octadecyl trimethyl ammonium salt) were chosen for this study due to their ability to withstand high temperature, good dispersion and the fact that they were well studied. The resin chosen for this work is Epon 862 which is a di-glycidyl ether of bisphenol-f with a moderately cured low viscosity aliphatic amine curing agent, Epikure 3274. Thermo-Gravimetric Analysis of the clay and their subsequent epoxy nanocomposites was studied. An improvement in the on-set of decomposition temperature and thermal stability of both the clays was found, their epoxy nanocomposites did not show any appreciable improvement in their degradation temperatures.

Samples were fabricated with 0.25 wt%, 0.5 wt%, 1.0 wt% and 2.0 wt% clay using magnetic mixing followed by using a high speed shear disperser. X-Ray Diffraction analysis was used in studying the dispersion of clay in the polymer. The fracture toughness of the composite samples was measured using SENB (Single End Notch Beam) test. It was observed that the critical stress intensity factor (K_{1C}) for the epoxy composites fabricated with Cloisite 20A and Nanomer I.28 E washed clay did not show any substantial improvement in the toughness. The flexural modulus was found to remain sililar for both the as-received and washed polymer based epoxy silicate composites. Morphology of the fractured specimens was studied using Scanning Electron Microscopic imaging. Aggregates were observed for composites fabricated with I.28 E as-received and washed clay/epoxy nanocomposites. Removal of excess surfactant is not a critical issue and did not have any effect on the thermal and mechanical properties of epoxy-clay nanocomposites.

ADVISOR'S APPROVAL: Dr.Raman P. Singh